Interpreting scattered in-situ produced cosmogenic nuclide depth-profile data

Kristell Le Dortz, Bertrand Meyer, Michel Sébrier, Regis Braucher, D. Bourles, L Benedetti, H. Nazari, M. Foroutan

Interpreting scattered *in-situ* produced cosmogenic nuclide depth-profile data

K. Le Dortz [1,2,3*], B. Meyer [1,2], M. Sébrier [1,2], R. Braucher [4], D. Bourlès [4], L. Benedetti [4], H. Nazari [5], M. Foroutan [1,2,5]

1- UPMC Univ Paris 06, ISTEP, UMR 7193, F-75005, Paris, France

2- CNRS, ISTEP, UMR 7193; F-75005, Paris, France

3 - Laboratoire de Géologie, ENS, UMR 8538, 75231 Paris

4 - *CEREGE, UMR 6635 CNRS-Aix Marseille Université, 13545 Aix-en-Provence, France*

5- Geological Survey of Iran, Teheran, Iran

*Corresponding author : Phone : 0033144322275, Fax : 0033144322200 Email : ledortz@geologie.ens.fr

Abstract

Modelling the evolution of the concentration of *in-situ* produced cosmogenic nuclides as a function of depth (depth-profile) has been developed to allow determining both the exposure duration and the denudation rate affecting geomorphic features. However, material sampled through surficial deposits may exhibit an inherited component resulting from exposure to cosmic rays before deposition. In case of homogeneous inheritance, this inherited component may be estimated through sampling at increasing depths and subsequently subtracted. In case of variable inheritance, the measured concentrations are scattered and the random distribution of the depth-profile concentrations prevents modelling confidently a depth-profile and precludes constraining an exposure duration. Often observed in desert and endorheic regions, this greatly restricts the possibilities to determine an accurate abandonment age of alluvial surfaces in such environments. Provided the denudation is demonstrated negligible, a method for determining a more accurate range of minimum inheritance, hence a more accurate maximum abandonment age for a given alluvial surface, is proposed. This method, based on the rejuvenation of depth-profile samples, relies on the simple hypothesis that at least one of the depth-profile samples would be emplaced with no or negligible inherited component and on the obvious principle that none of analyzed sample has been emplaced with a negative

cosmogenic nuclide concentration. The method consists then in determining which of the measured depth-profile sample may have been emplaced with a null CRE concentration; i.e., with a zero inheritance value. This requires to calculate the *in-situ* duration of exposure needed to reach the concentration measured for each depth-profile sample and to retain the one that provides the smallest *in-situ* exposure duration. Several examples from alluvial surfaces of central Iran illustrate the profile rejuvenation method and highlight a variable inheritance ranging between $1.5x10^5$ and $16.1x10^5$ at/g (SiO_2) for terraces whose abandonment ages range from ten to several hundreds of ka.

Introduction

Cosmic ray exposure (CRE) dating has been widely used to estimate the age of alluvial surfaces in many regions worldwide. For a long while and still for some recent studies, surface samples only were collected to determine CRE ages (e.g., Ritz et al., 1995, Regard et al., 2006, Van der Woerd et al., 2006). Measurement of their cosmogenic nuclide concentration (most often ^{10}Be) yields a CRE age for each collected pebble (Figure 1a, upper panel). If enough pebbles have been collected on a given surface, a suitable statistical treatment may exhibit a Gaussian distribution centred on the weighted mean age eventually assigned to the studied surface (Figure 1b, upper panel). Sometimes, the measured concentrations are scattered and their distribution is multimodal (Figure 1c, upper panel). The occurrence of outliers resulting either from pre- or post-depositional processes is thus extensively discussed. While some authors point to denudation and artificial rejuvenation of the surface and favour the oldest ages (e.g., Brown et al., 2005), others point to inheritance and artificial ageing of the surface and therefore favour the youngest ages (e.g., Mériaux et al., 2005; Vassallo et al., 2007). Pre-depositional exposure indeed implies the accumulation of an inherited component that shifts the final Gaussian distribution towards greater concentrations while post-depositional denudation brings to the surface less concentrated sub-surface pebbles that widens and shifts the Gaussian distribution towards smaller concentrations. Neither the inherited component, nor the denudation rate can be estimated using surface samples only. In an attempt to clear up this point, depth-profile sampling has often been undertaken (Figure 1a, lower panel). Providing that the material constituting the deposit of interest has been emplaced over a short period of time, some ka, with respect to the subsequent duration of exposure and that it has been homogeneously pre-exposed, the depth-profile samples, whether individual or amalgamated pebbles, exhibit an exponential decrease

of their concentration as a function depth controlled by the attenuation length of the producing particles (e.g., Anderson et al., 1996; Repka et al., 1997). An exponential tending asymptotically to zero indicates no inherited component, while an exponential tending asymptotically to a characteristic concentration indicates a homogeneously distributed inherited component whose concentration is given by the asymptotically reached value (Figure 1b, lower panel). A chi-square inversion minimising the difference between the measured and modelled concentrations is often used to constrain from these depth-profiles the exposure duration of the studied surfaces, their denudation rate, and the concentration of their inherited components, if homogeneous (e.g., Siame et al., 2004; Braucher et al., 2009). Where the number of surface samples is limited or the distribution of their concentrations multimodal, depth-profiles also help narrowing the range of possible surface ages (e.g., Nissen et al., 2009; Champagnac et al., 2010). However, scattered surface pebble concentrations are sometimes observed together with random depth distributions of ^{10}Be concentrations (e.g., Le Dortz et al., 2009). In such cases (Figure 1c), the distribution of surface pebbles is multimodal and the concentrations of the depth-profile samples do not decrease exponentially with depth, suggesting a variable inheritance and making any conventional modelling useless.

We have investigated such situations encountered in the desert region of central Iran while analysing offset fan surfaces along the Dehshir (Le Dortz et al., 2011) and Anar (Le Dortz et al., 2009) faults. Although sands appear to be less sensitive to inheritance than gravels (e.g., Matmon et al., 2005; Schmidt et al., 2011), the overall low sand content in the investigated alluvial material precluded the possibility to perform depth profile analysis on sandy material. Consequently, it was appropriate to collect samples of comparable granulometries (pebbles and cobbles) on the surface and all along depth-profile. To account for the scattering of cosmogenic nuclide concentrations and to determine the possible ranges of both the abandonment ages of the analyzed fan surfaces and the inheritance carried by their gravels, a CRE procedure has been developed. This procedure is based on depth-profile analyses, whose results are subsequently compared to the overlying surface samples. Such a procedure reveals appropriate because the studied sites met two necessary conditions: (1) the negligible denudation rate of the fan surface implies that depth-profile concentrations only depend on two unknowns (pre-exposure and *in-situ* exposure), and (2) the common source of alluvial material for both the surface and depth-profile samples implies that depth-profile samples can be compared with surface ones. The scatter of the measured cosmogenic nuclide concentrations resulting thus only from a variable inheritance, the concentrations calculated

using the proposed depth-profile rejuvenation procedure allow estimating a maximum abandonment age for a given fan surface and provide a range of minimum inheritance. The complete description of the sites, the sampling strategy, the details of the performed analyses, and the modelled ages can be retrieved in two previous papers (Le Dortz et al., 2009; Le Dortz et al., 2011). Some of these pebble data are used here to illustrate and discuss the limitations of a method, the profile rejuvenation procedure, which accounts for the variability of inheritance where denudation is negligible.

1. Profile rejuvenation methodology.

Scattering of cosmogenic nuclide surface concentrations at a given site may result from both denudation processes and/or variable inheritance. At the Dehshir and Anar sites, qualitative observations of a desert pavement covering the very pristine surface of the fans made of varnished clasts suggested low erosion rate. This is quantitatively confirmed measuring the concentrations of two distinctive cosmogenic nuclides having different half-lives, ^{10}Be (1.387 Ma; Chmeleff et al., 2010, Korschinek et al., 2010) and ^{36}Cl (0.301 Ma; e.g., Gosse & Philipps, 2001) in samples along depth-profiles from the same oldest surface. The ^{36}Cl ages calculated assuming no denudation and no inheritance are systematically younger than the ^{10}Be ages calculated under the same assumptions, indicating that the carbonates samples had nearly reached the steady-state equilibrium - cosmogenic nuclide production balanced by losses due to radioactive decay and denudation, if any - at which the ^{36}Cl concentration only depends on the denudation rate. Modelling then the evolution of the ^{36}Cl concentrations along the depth-profiles quantitatively confirmed a denudation rate lower than 10^{-3} mm.yr^{-1}, hence negligible, over the investigated time span (Le Dortz et al., 2011).

Even if denudation rate is negligible, the original distribution of the pebbles at the surface of a terrace may be modified since their abandonment on the tread due to their closeness to the risers between two terrace levels, local overfloodings (e.g., Van der Woerd et al., 1998) or surface runoff, and diffusion (Owen et al., 2011). Sampling far from the risers may help mitigating such effects. However, one cannot rule out that a few of the pebbles collected at the surface might have been brought by animals or shepherds either from higher or lower, hence older or younger, levels. Such modifications are excluded for material deeper in a terrace. Unless biopedoturbation, ploughing or cryoturbation has modified the original relative depth position of some pebbles within the terrace material (Frankle et al., 2011), the samples collected at depth do represent the original relative depth distribution of the terrace

material. Clearly, there is no evidence for significant biopedoturbation, ploughing, or cryoturbation in the desert environment prevailing in central Iran. If it were, amalgamating 10-30 individual pebbles for each depth-profile sample would ensure diluting the contributions of a few anomalous pebbles. Considering all the above-mentioned remarks, the scatter of cosmogenic nuclide concentrations (Figure 2a) measured both at the surface and along depth-profiles at several sites in central Iran should only result from two unknown contributions: the *in-situ* cosmogenic nuclide production and the pre-exposure of the analyzed samples. To limit these contributions, we propose to determine the minimum range of inheritance of a terrace, and consequently its maximum abandonment age, analyzing first the depth-profile samples. Providing that the terrace aggraded during a short time interval coeval with a single climatic crisis, as confirmed by OSL ages within some of the alluvial terraces (Le Dortz et al., 2011) and was not subsequently affected by significant denudation, the measured depth-profile concentrations should only result from *in-situ* production and pre-exposure. Then the proposed method relies on the impossibility for any depth-profile samples to have been emplaced in the terrace material with a negative cosmogenic nuclide concentration. Thus, considering the sampling depth and assuming that the measured concentration would only results from *in-situ* production (i.e., the sample would have been emplaced with a null cosmogenic nuclide concentration), one can calculate the time needed to bring back to zero each depth-profile concentration. The maximum abandonment age corresponds to the time needed for the depth-profile sample, which could be brought back from its measured concentration to a null concentration without bringing the other depth-profile samples to a negative concentration (Figure 2b, step 1). Therefore, this method is based on the simple hypothesis that, if denudation is negligible, at least one of the depth-profile samples could be emplaced with no inherited component. Subtracting for each profile sample the concentration accumulated at its sampling depth during the thus estimated maximum abandonment age to the measured concentration yields excess concentrations that correspond, when corrected for radioactive decay since the maximum abandonment age, to the minimum inherited components

The accuracy of the maximum abandonment age deduced from the profile rejuvenation method may then be evaluated through its comparison with the abandonment ages deduced from the concentrations measured in the individual pebbles or cobbles collected on the terrace tread. However, a prerequisite to such comparison is to ensure that the material sampled at a given site along a depth-profile and on the fan surface originates from the same source. For two (Anar and Dehshir North) out of three of the analyzed sites, the geologically

homogeneous catchment areas are small enough to reasonably postulate a short transport duration of the alluvial material. In addition, approximately 4-m-high natural or excavated outcrops within the alluvial sediments do not evidence significant change of gravel source during the fan aggradation. Thus, it is qualitatively unlikely that the source of the alluvial material changed during the emplacement of the near-surface and surface samples. To validate these field observations, an *a posteriori* statistical comparison of the concentrations measured at the surface with those measured along depth-profiles was performed at each analyzed site (see Appendix and following sections). The maximum abandonment age determined using the profile rejunevation method allows calculating a maximum surface concentration at each given sampling site according to its spatial coordinates. Adding that maximum concentration to that found in excess in each profile sample, when using the same rejuvenation procedure (see above), yields to surface equivalent calculated concentrations that thus represent the concentrations that would have been measured if the samples collected along the depth-profile had been exposed solely at the surface. Finally, these calculated values are compared to the concentrations measured in the surface samples. Because nearly all the calculated concentrations fall in the range of those measured at the surface this implies that samples from depth-profiles and surfaces originate at each site from the same source. Therefore, we consider that the amalgam depth-profile concentrations represent the average concentration that would yield multiple sampling of pebbles at a given depth and the scatter of concentrations between successive amalgams corresponds mainly to the variability of inheritance among a homogeneous source. This scatter of concentrations along depth-profiles corresponds then only to variable pre-exposure duration in the upper catchments, and the accuracy of the maximum abandonment age of the fan surface determined using the profile rejuvenation method may thus be compared to the surface concentrations (Figure 2c, step 2). Thus, if most concentrations of the surface pebbles become negative while subtracting the *in-situ* concentration that would have been accumulated at the surface during the duration that corresponds to the maximum cosmogenic nuclide abandonment age determined from the profile rejuvenation, then that maximum abandonment age is not physically acceptable (Figure 2c, right). On the contrary, if most of these surface concentrations remain positive by performing the same operation, the maximum cosmogenic nuclide abandonment age (t_{Max}) provides a maximum possible age for the fan surface (Figure 2c, left).

Finally, a minimum cosmogenic nuclide abandonment age (t_{min}) can be estimated from the lowest surface concentration (Figure 2d, step 3) that, in addition, allows estimating the maximum range of inheritance values for such a t_{min}. This minimum cosmogenic nuclide

abandonment age may be compared with OSL ages, if available, to discuss whether it still could be affected by some inherited component. The following examples highlight the variability of the inheritance and illustrate the methodology to account for this variability and derive accurate limits on the inheritance and hence on the possible range of abandonment ages of a given alluvial terrace unaffected by denudation.

2. Estimating the ranges of inheritance and abandonment age on an alluvial terrace

To illustrate the principles of the proposed methodology, samples from an intermediate terrace emplaced by the Marvast river at the Iranian Dehshir South site (T2 terrace; Le Dortz et al., 2011) are used (Figure 3a, left). Seven surface samples have been analysed and their calculated ^{10}Be age distribution is multimodal. Discarding the possible outlier DS08S114 (49.9 ± 3.3 ka), their weighted mean ^{10}Be age is of 175 ± 62 ka (Table 1, Figure 3a, right). In order to try to better constrain the abandonment age of this alluvial deposit, seven samples were taken at increasing depths along a 4-m profile. Each sample is an amalgam of 10-30 pebbles aiming at measuring the mean concentration at each level. The random evolution of the measured ^{10}Be concentrations as a function of depth does not permit to plainly model the obtained depth-profile and hence to define a limiting isochron as theoretically proposed by Ryerson et al. (2006). This random distribution excludes uniform pre-exposure of the material, prior to its emplacement as the T2 alluvial terrace, and suggests thus variable inheritance. Recent work dealt with the occurrence of variable inheritance in alluvial terraces (e.g., Schmidt et al., 2011). In the latter, a variable inheritance is evidenced only in boulders collected on the surface while concentration of sand samples decrease exponentially along a depth-profile, suggesting a homogeneous inheritance. Schmidt et al. (2011) suggest that the differences in the inherited component are related to the different provenances and pre-exposure histories of the different material. In our case, the variability of inheritance is observed for pebbles and cobbles of different nature (quartz for ^{10}Be and carbonates for ^{36}Cl) for which internally coherent results have been obtained on a same terrace (Le Dortz et al., 2011). The method described in section 1 was thus used to account for the variability and derive accurate bounds on the minimum inheritance.

The performed analysis indicates that terrace T2 was abandoned at most 107 ka ago, that is the time required to bring sample P127 concentration back from its current value to zero without bringing back any other depth-profile sample to a negative concentration (Figure 3b). The concentration in excess remaining after subtracting to the measured concentration the concentration accumulated by *in-situ* production during 107 ka at the sampling depth

239 corresponds for all samples but P127 to the decay of the original inherited component (Table
240 A.1). Concentration in excess are ranging from $2.15x10^5$ at/g(SiO_2) (sample P126) to
241 $7.86x10^5$ at/g(SiO_2) (sample P130). After correcting for the radioactive decay during the last
242 107 ka, the inherited concentrations corresponding to the maximum abandonment age of the
243 T2 terrace (Table A.1) are ranging from $2.27x10^5$ to $8.29x10^5$ at/g(SiO_2). As mentioned
244 previously, one has to demonstrate that the depth-profile samples and the surface samples
245 originated from the same source area. As discussed above, summing the surface concentration
246 accumulated during 107 ka exposure duration to each concentration in excess determined for
247 the depth samples (see Appendix and Table A.1) yields to depth-profile derived surface
248 concentrations within the range of those measured in the surface samples (Figure A.1).
249 Moreover, the other possible abandonment ages based either on the lowest surface
250 concentration (minimum cosmogenic nuclide abandonment age of 50 ka) or even on the OSL
251 ages (≈ 30ka) yield similar conclusions. Thus, all these statistical considerations demonstrate
252 *a posteriori* that the gravels of the depth-profile and the ones of the fan surface sample
253 originate from the same variably pre-exposed source and can thus be compared. Regarding
254 the surface samples, the profile rejuvenation method using the concentration accumulated at
255 the surface by *in-situ* production during 107 ka brings only one of the surface samples to a
256 negative concentration (Figure, 3b). This remains acceptable as this sample is, in addition, the
257 statistical outlier DS08S114. It is nonetheless important to notice that this age of 107 ka is the
258 uppermost bound for the abandonment age and thus for the *in situ* exposure duration.
259 Consequently, exposure ages ranging from 0 to 107 ka are theoretically possible for the T2
260 surface. On the one hand, exposure ages ranging between 53 ka (oldest possible age of the
261 youngest sample, DS08S114, Table 1) and 107 ka would make that statistical outlier younger
262 than the age of the terrace. On the other hand, exposure ages ranging between zero and 53 ka
263 would be compatible with the occurrence of the statistical outlier as well as the other surface
264 samples collected on T2. All exposure ages younger than 47 ka (youngest possible age of the
265 youngest sample, DS08S114, Table 1) would imply that the youngest sample collected at the
266 surface has a significant inherited component. At this location, two OSL ages yielded
267 26.9±1.3 ka at 0.8 m depth and 29.4±5.1 ka at 3.4 m depth, suggesting that the terrace
268 material aggraded on a short period of time and that the youngest CRE sample may still
269 contain some inheritance.
270 Because surface sampling does not allow accounting for inheritance, while profile
271 rejuvenation permits retrieving the range of variable inheritance, the age range of 175±62 ka
272 obtained considering the sole surface samples is incompatible with the maximum cosmogenic

nuclide abandonment age deduced from the depth profile samples analysis. As a consequence, the lowest surface concentration (DS08S114, Table 1) measured in the statistical outlier, provides a realistic minimum cosmogenic nuclide abandonment age of 50 ± 3 ka. This T2 minimum abandonment age yields to maximum inheritance ranging between 3.29×10^5 and 8.59×10^5 at/g (Figure 3c and Table A.1). Selecting a youngest abandonment age derived from the OSL ages would increase very slightly the inheritance without changing the overall figure (see Table A.1).

Therefore, the cosmogenic nuclide abandonment ages range for T2 abandonment should be narrowed to 47-107 ka and the alluvial material appears to have emplaced with inherited concentrations ranging from 2.27×10^5 to 8.7×10^5 at/g.

3. Case study

3.1 Example of an old terrace

In the same region (Figure 4a, left), the ^{10}Be concentrations measured along a depth-profile from a higher, hence older, terrace (T3; see Le Dortz et al., 2011) were analysed. The *in-situ* produced ^{10}Be concentrations increasing with the exposure duration and the ^{10}Be inherited concentrations radioactively decreasing, it can be anticipated that the proportion of *in-situ* produced ^{10}Be with respect to the inherited one increases with the abandonment age. The longer is the *in-situ* exposure duration, the higher is the dilution of inheritance. Ten quartz samples were collected on the T3 tread (Table 1 and Figure 4a, right). The distribution of these surface CRE ages, considering sample DN06S2 (235.5 ± 35.4) as an outlier, is unimodal and leads to a weighted mean CRE age of 462 ± 55 ka. Amalgamated samples have also been collected along a depth-profile. Their ^{10}Be concentrations exhibit an overall exponential decrease with depth but the deepest sample displays nonetheless a much higher concentration than the two samples above it. Such a ^{10}Be depth-profile can theoretically be modelled (pink curve, Figure 4b). The best fit, assuming no denudation, is obtained for an abandonment age of 464 ka and a homogeneous inheritance of 3.8×10^5 at/g (SiO_2), which would correspond to a pre-exposure duration of ~32 ka, if acquired at the surface in conditions similar to that at the Dehshir North site (Le Dortz et al., 2011). One may find satisfactory the coherence between the abandonment ages deduced from the surface samples and the modelling of the depth-profile samples. However, the fact that the inherited concentration derived from the modelling of the depth-profile is half the concentrations measured for the deepest samples is intriguing, and opens the possibility for the occurrence of

variable inheritance. As for T2, the methodology described to estimate the minimum inheritance considering only the depth-profile samples has thus been applied to T3.

For T3, the depth-profile sample, whose concentration can be restored to zero by subtracting a simple *in-situ* exposure duration at the sampling depth without bringing back any other depth-profile sample to a negative concentration, is P12 (Figure 4b and Table A.1). The minimum excess concentration (2.43×10^5 at/g (SiO_2)) is obtained for sample P17, collected at 2.7 m depth, and the maximum excess concentration (9.04×10^5 at/g (SiO_2)) is obtained for sample P14. Accounting for the radioactive decay, this brackets the minimum inherited component between 2.99×10^5 and 11.1×10^5 at/g.

The maximum cosmogenic nuclide abandonment age of 412 ka deduced from the profile rejuvenation method agrees with the range of abandonment ages deduced from surface samples only (462 ± 55 ka). This consistency is significant when considering that summing the surface concentration accumulated during 412 ka exposure duration to each concentration in excess determined for the depth samples yields to depth profile derived surface concentrations within the range of those measured in the surface samples (see Appendix, Figure A.2 and Table A.1). This allows narrowing the abandonment age interval to 407-412 ka. It is worth noticing that this rejuvenation would yield only one of the surface samples to a negative concentration, the statistical outlier DN06S2 (Figure 4b). All the other such rejuvenated surface samples display positive excess concentrations. While abandonment ages for the terrace T3 older than 412 ka are not possible because they would imply a negative concentration for at least one depth-profile amalgam (P12), younger exposure ages remain possible. Theoretically, all exposure ages ranging between 0 and 412 ka are possible. On the one hand, exposure ages ranging between 271 ka (oldest possible age of the youngest T3 surface sample DN06S2, Table 1) and 412 ka would make that statistical outlier younger than the age of the terrace. On the other hand, exposure ages ranging between zero and 200 ka (youngest possible age of the youngest T3 sample DN06S2, Table 1) would be compatible with the occurrence of the statistical outlier as well as the other surface samples collected on T3. All ages younger than 200 ka would imply that the youngest surface sample also contains some inheritance.

One may therefore consider the youngest surface sample -i.e., the statistical outlier DN06S2 (235.55±35.38 ka) - as the last pebble emplaced on the T3 tread before its abandonment and subsequent incision. Considering the possibility for a variable inheritance as for T2, the age of sample DN06S2 might be closer to the abandonment age of surface T3. If the concentration corresponding to 235 ka of *in-situ* production at their sampling depth is

subtracted to each surface and depth-profile sample, the age distribution of such rejuvenated surface samples remains unimodal (Figure 4c, top). However the concentrations of the "rejuvenated" depth-profile samples remain too scattered to allow for a simple profile modelling, revealing that inheritance is not homogeneous (Figure 4c, bottom). The minimum abandonment age of 235 ka, which is calculated for T3, permits to estimate the range of the variable maximum inheritance. Accounting for the radioactive decay, the range of the maximum inheritance between 3.62×10^5 and 16.12×10^5 at/g appears rather large (Table A.1). This case study illustrates that an unknown and variable inheritance can always be modelled as a homogeneous inheritance once the portion of the concentration that has been acquired at the sampling depth since the deposit emplacement becomes significantly larger than that inherited from surface pre-exposure.

3.2 Example of a young terrace

A similar approach has been applied to the surface and depth-profile samples of a young terrace level (the T1 terrace offset by the Anar fault along the western piedmont of the Kuh-e-Bafq about 150 km east of the Dehshir sites, Figure 5a, left; see Le Dortz et al., 2009). For a young terrace, the proportion of inherited concentration, if there is any, may be large with respect to the *in-situ* produced concentration acquired at the sampling depth since the deposit emplacement. Ten quartz samples and seven amalgamated samples were collected on the surface and along a depth-profile through a well-defined abandoned fan surface, respectively (figure 5). The CRE ages of the surface samples are scattered and display a multimodal distribution with a weighted mean CRE age of 32 ± 25 ka (Figure 5a, right). This terrace appears significantly younger than the ones studied in the Dehshir area. The error-bars on the mean value are too large to allow tightly constraining an abandonment age. The distribution of depth-profile concentrations is random, dismissing a homogeneous pre-exposure prior to the emplacement of the fan material (Figure 5b). Besides, the deepest depth-profile samples display ^{10}Be concentrations larger than that of many of the surface samples. This exemplifies the occurrence of a variable inheritance and led Le Dortz et al. (2009) to approximate the abandonment age of the terrace by that of the youngest pebble.

Applying the rejuvenation method described above to the depth-profile samples yields a maximum cosmogenic nuclide abandonment age of 46 ka, which implies minimum excess concentrations ranging from 0.7×10^5 to 4.16×10^5 at/g (SiO_2) (Figure 5b and Table A.1). Summing the surface concentration accumulated during 46 ka exposure duration to each concentration in excess determined for the depth samples indeed yields to depth-profile

derived surface concentrations that are not fully compatible with those measured in the surface samples (see Appendix, Table A.1 and Figure A.3). In addition, applying this maximum cosmogenic nuclide abandonment on surface samples implies that all but one of the rejuvenated surface samples would display negative concentrations, highlighting that the maximum cosmogenic nuclide abandonment age of 46 ka deduced from the rejuvenation of the depth-profile data is largely overestimating the actual abandonment age of the terrace. Minimum inheritance must then be higher than those estimated using the profile rejunevation method, which prevents determining a maximum cosmogenic nuclide age. The abandonment age of the alluvial surface is thus better approximated by the CRE age of the youngest surface sample (17.5 ± 1.1 ka; sample AS06S75 in Table 1). Subtracting a concentration corresponding to a simple exposure duration of 17.5 ka at their sampling depth, one verifies that none of the depth-profile sample has been emplaced with a negative concentration (Figure 5c). This minimum CRE age of 17.5 ka permits to calculate a range of maximum inheritance bracketed between 1.48×10^5 and 4.30×10^5 at/g (SiO_2). This confirms that the ^{10}Be concentration of the deepest sample (P97) results nearly entirely from inheritance whatever the range of theoretical exposure age (0-46 ka). It is nonetheless possible that the youngest surface sample concentration also incorporates some inheritance. This is the case for this studied Anar site as demonstrated by OSL burial ages associated to samples collected below the tread (5.8±3.6 ka at 0.8 m depth and 14.4±3.9 ka at 4.1 m depth) that are younger than the CRE ages of pebbles collected on the tread (Le Dortz et al., 2009). Interestingly summing the surface concentration accumulated during either 17.5 ka (youngest CRE age) or 10 ka (average OSL age of the final fan aggradation) exposure duration to each corresponding concentration in excess determined for the depth samples yields to depth profile derived surface concentrations that are compatible with those measured in the T1 surface samples (see Appendix, Table A.1 and Figure A.3). This again demonstrates that the depth-profile and surface samples originate from the same source. Therefore, this case study illustrates the limitation of the profile rejuvenation method for very young alluvial surfaces (0-20 ka) for which, the portion of variable inheritance is significant with respect to the proportion of the concentration acquired at the sampling depth since the deposit emplacement. In such conditions, it appears more pertinent to rely on the youngest surface sample to approximate the age of the surface.

Conclusion

The profile rejuvenation method allows handling the complications raised by variable inheritance when using *in-situ* produced cosmogenic nuclide concentrations in regions where denudation is demonstrated negligible, a necessary condition which limits the unknowns to the *in-situ* exposure duration and to the inherited component resulting from pre-exposure. This approach is illustrated by analyses of samples collected from alluvial terraces in the arid environment of the central Iran plateau where denudation has been demonstrated negligible (Le Dortz et al., 2011). Where depth-profiles cannot be modelled to determine a homogeneous inheritance, this profile rejuvenation procedure may allow to derive from the depth-profile samples a maximum cosmogenic nuclide abandonment age for the surface of an alluvial terrace and to estimate a range of minimum inherited concentrations. The consistency between the surface and depth profile concentrations has to be checked for each site to ensure that both surface and depth profile samples originate from the same source (see Appendix). When the profile rejuvenation method yields negative concentrations for most of the surface samples, this indicates that the profile derived maximum abandonment age significantly overestimates the actual surface abandonment age. As a consequence, the youngest of the surface samples appears as the best approximation for the abandonment age of the alluvial terrace rather than the weighted mean CRE age of many samples. This youngest age provides the minimum abandonment age based on CRE data and permits to calculate a range of maximum inheritance. Interestingly, this was empirically formulated for Holocene terraces at some places in Mongolia (Vassallo et al., 2007) and at some sites along the southern rim of the Tarim basin (Mériaux et al., 2005). The different sites we analyzed in the desert environment of central Iran show that the procedure of rejuvenation profile allows handling the variable inheritance of alluvial material whatever the age of the analyzed terrace. In central Iran, where variable inheritance is observed, the inherited concentrations range between 1.48 $x10^5$ and $16.1x10^5$ at/g. However, the range of inheritance for a given site is much smaller, the inheritance concentrations varying approximately in a ratio 1-3. In addition, the maximum inheritance values appear to increase with terrace abandonment ages. Nevertheless, we do not have enough sites to ascertain such conclusion and this observation may only reflect difference in catchments and/or in pre-exposure processes. If the observed inheritances would have accumulated at the surface, they would be equivalent to CRE duration ranging from 15 ka to 130 ka.

The occurrence of such high, inherited concentrations for the sites analyzed in central Iran may result from the endorheic drainage of the Iranian plateau that prevents significant fluvial incision (Le Dortz et al., 2009). Thus, low denudation rates and weak incision favour

the feeding of alluvial fans or terraces by reworking older alluvial material. As a consequence, this older alluvial material has been previously exposed to cosmic rays and carries a variable amount of inheritance according to the depth where it was eroded and/or the number of times it was reworked. This alluvial "cannibalism" may also characterize many arid endorheic regions such as Altiplano, central Asia (Tarim, Mongolia, Tibet…), where the amount of denudation is thought negligible. Therefore, this method could be usefully applied to analyze the cosmogenic nuclide concentrations in such regions to determine bounds of maximum *in-situ* CRE duration and ranges of inheritance.

Even more interesting than the important amount of inheritance is the high variability of that inheritance expressed by the random distribution of the concentrations of the amalgams along a given profile. Indeed, smaller variations between two successive samples amalgamating 10-30 pebbles at a given depth are expected, anticipating they average the cosmogenic nuclide concentrations at that depth. The variability among amalgams may thus represent sudden and uneven episodes of aggradation of material exhumed from different places of the upper catchments. This would explain a rapid aggradation of the fanglomerates together with the lack for exponential decrease of the concentrations with depth. These observations may result from the fact the cosmogenic nuclide concentrations, which built up in landscape, are not completely reset by erosional climatic crisis. As a consequence, OSL ages may help constraining the history of alluvial aggradation (e.g., Le Dortz et al., 2009 and 2011; Fruchter et al., 2011; Guralnik et al, 2011). Finally, this study demonstrates the usefulness of combining both surface and depth-profile sampling either to approach confidently the abandonment age of alluvial fans or to document their aggradation history.

Acknowledgments:

This study benefited from initial funding by PNTS and 3F INSU programs. Université Pierre et Marie Curie (UPMC) and Geological survey of Iran (GSI) provided the complementary funding and the logistic assistance. KL received a Ministry of Research and Education scholarship granted by the President of UPMC. The ^{10}Be measurements were performed at the ASTER AMS national facility (CEREGE, Aix en Provence) that is supported by the INSU/CNRS, the French Ministry of Research and Higher Education, IRD, and CEA. L. Leanni, F. Chauvet, M. Arnold and G. Aumaître are acknowledged for their help during chemistry and measurements. We acknowledge Ari Matmon and one anonymous reviewer for constructive remarks that helped to greatly improve our manuscript.

References

Anderson, R.S. ; Repka, J.L. ; Dick, G.S., 1996. Explicit treatment of inheritance in dating depositional surfaces using *in-situ* 10Be and 26Al; Geology 24:47-51

Braucher, R., P. Del Castillo, L. Siame , A.J. Hidy , D.L. Bourlès., 2009. Determination of both exposure time and denudation rate from an *in-situ*-produced ^{10}Be depth profile : A mathematical proof of uniqueness. Model sensitivity and applications to natural cases. *Quaternary Geochronology* Volume 4, Issue 1, Pages 1-82

Brown, E.T., Molnar, P., and Bourlès D.L., 2005. Comment on "Slip-Rate Measurements on the Karakorum Fault May Imply Secular Variations in Fault Motion" Science 309 (5739), 1326b. [DOI: 10.1126/science.1112508].

Champagnac, J.-D., D.-Y. Yuan, W.-P. Ge, P. Molnar, and W.-J. Zheng., 2010. Slip rate at the northeastern front of the Qilian Shan, China, Terra Nova, 22, 180-187.

Chmeleff, J., von Blackenburg, F., Kossert, K., Jackob, D., 2010. Determination of the ^{10}Be half-life by multicollector ICP-MS and liquid scintillation counting. *Nuclear Instruments and Methods in Physics Research* B, **268**, 192–199.

Frankel, K.L., Dolan, J.F., Owen, L.A., Ganev, P.N., and Finkel, R.C., 2011, Spatial and temporal constancy of seismic strain release along and evolving segment of the Pacific-North America plate boundary: Earth and Planetary Science Letters, doi:10.1016/j.epsl.2011.02.034

Fruchter, N., Matmon, A., Avni, Y., Fink, D., 2011. Revealing sediment sources, mixing, and transport during erosional crater evolution in the hyperarid Negev Desert, Israel. Geomorphology 134, 363–377

Gosse, J.C., and Phillips, F.M., 2001, Terrestrial in-situ cosmogenic nuclides: theory and application:. Quaternary Science Reviews, v. 20, p. 1475-1560

Guralnik, B., Matmon, A., Avni, Y., Porat, N., Fink, D., 2011. Constraining the evolution of river terraces with integrated OSL and cosmogenic nuclide data. Quat. Geochron. 6, 22–32.

Korschinek, G., Bergmaier, A., Faestermann, T., Gerstmann, U. C., Knie, K., Rugel, G., Wallner, A., Dillmann, I., Dollinger, G., Lierse von Gosstomski, Ch., Kossert, K., Maiti, M., Poutivtsev, M., Remmert, A., 2010. A new value for the ^{10}Be half-life by Heavy-Ion Elastic Recoil detection and liquid scintillation counting. *Nuclear Instruments and Methods in Physics Research* B, **268**, 187–191.

Le Dortz, K. Meyer B., Sébrier M., Nazari H., Braucher R., Fattahi M., Benedetti L., Foroutan M., Siame L., Bourles D., Talebian M., Bateman M.D. and Ghoraishi M., 2009. Holocene right-slip rate determined by cosmogenic and OSL dating on the Anar fault, Central Iran. Geophysical Journal International, **179,** 700–710, doi : 10.1111/j.1365-246X.2009.04309.x

Le Dortz, K. Meyer B., Sébrier M., Braucher R., Nazari H., Benedetti L., Fattahi M., Bourles D., Foroutan M., Siame L., Rashidi, A., Bateman M.D., 2011. Dating inset terraces and offset fans along the Dehshir fault combining cosmogenic and OSL methods. Geophysical Journal International, 185**,** 1147-1174, DOI: 10.1111/j.1365-246X.2011.05010.x

Matmon, A., Schwartz, D.P., Finkel, R., Clemmens, S., Hanks, T., 2005. Dating offset fans along the Mojave section of the San Andreas fault using cosmogenic 26Al and 10Be. Geol. Soc. Am. Bull. 117, 795–807.

Mériaux, A.-S., Tapponnier, P. Ryerson, F. J. Xiwei, X. King, G. Van der Woerd, J. Finkel, R. C. Haibing, L. Caffee, M. W. Zhiqin, X., 2005. The Aksay segment of the northern Altyn Tagh fault: Tectonic geomorphology, landscape evolution, and Holocene slip rate, *J. Geophys. Res.*, **110**, B04404

Nissen, E., Walker R.T., Bayasgalan B., Carter A, Fattahi M., Molor E., Schnabel C., West A. J., Xu S., 2009. The late Quaternary slip-rate of the Har-Us-Nuur fault (Mongolian Altai) from cosmogenic ^{10}Be and luminescence dating, *Earth Planet. Sci. Lett.* 286, 467-478, doi:10.1016/j.epsl.2009.06.048

Owen, L.A., Frankel, K.L., Knott, J.R., Reynhout, S., Finkel, R.C., Dolan, J.F., Lee, J., 2011. Beryllium-10 terrestrial cosmogenic nuclide surface exposure dating of Quaternary landforms in Death Valley. Geomorphology 125, 541–557 doi:10.1016/j.geomorph.2010.10.024.

Regard, V., O. Bellier, R. Braucher, F. Gasse, D. Bourlès, J. Mercier, J.-C. Thomas, M.R. Abbassi, E. Shabanian and Sh. Soleymani, 2006. ^{10}Be dating of alluvial deposits from Southeastern Iran (the Hormoz Strait area), *Palaeogeography, Palaeoclimatology, Palaeoecology*, 242, 36-53.

Repka, J. L., R. S. Anderson and R. C. Finkel, 1997. Cosmogenic dating of fluvial terraces, Fremont River, Utah; Earth and Planetary Science Letters 152:59-73

Ritz, J.F., Brown, E.T., Bourlès, D.L., Philip, H., Schlupp, A., Raisbeck, G.M., Yiou, F., and Enkhtuvshin, B. 1995. Slip rates along active faults estimated with cosmic-ray-exposure dates: Application to the Bogd fault, Gobi- Altaï, Mongolia. Geology 23: 1019-1022.

545 Ryerson, F.J., Tapponnier, P., Finkel, R.C., Meriaux, A., Van der Woerd, J., Lasserre, C.,
546 Chevalier, M., Xiwei, X., Haibing, L., King, G.P., 2006. Applications of
547 morphochronology to the active tectonics of Tibet. *GSA, Special Papers*, **415**, 61-86,
548 doi: 10.1130/2006.2415(05)
549 Schmidt, S., Hetzel, R., Kuhlmann, J., Mingorance, F., Ramos, V.A., 2011. A note of caution
550 on the use of boulders for exposure dating of depositional surfaces. *Earth and*
551 *Planetary Science Letters*, **302**, 60-70. doi: 10.1016/j.epsl.2010.11.039.
552 Siame, L., O. Bellier, R. Braucher, M. Sebrier, M. Cushing, D. Bourlès, B. Hamelin, E.
553 Baroux, B. de Voogd, G. Raisbeck, F. Yiou, 2004. Local erosion rates versus active
554 tectonics : cosmic ray exposure modelling in Provence (south-east France). *Earth*
555 *Planet. Sci. Lett*, **220**, 3-4, 345-364.
556 Stone J. O., 2000. Air pressure and cosmogenic isotope production. J. Geophys. Res.,105,
557 B10, 23753-23759.
558 Van der Woerd, J., F. J. Ryerson, P. Tapponnier, Y. Gaudemer, R. C. Finkel, A.-S. Meriaux,
559 M. W. Caffee, G. Zhao, and Q. He, 1998. Holocene left slip-rate determined by
560 cosmogenic surface dating on the Xidatan segment of the Kunlun fault (Qinghai,
561 China), Geology 26,695 –698.
562 Van der Woerd, J., Klinger Y., Sieh K., Tapponnier P., Ryerson F.J., Mériaux A-S., 2006.
563 Long-term slip rate of the southern San Andreas fault from 10Be-26Al surface exposure
564 datation of an offset alluvial fan, J. Geophys. Res, 111, B04407.
565 Vassallo R, Ritz J, F., Braucher R, Jolivet M, Carretier S, Larroque C, Chauvet A, C. Sue C,
566 Todbileg M, Bourlès D, Arzhannikova A, Arzhannikov S., 2007. Transpressional
567 tectonics and stream terraces of the Gobi-Altay, Mongolia. Tectonics 26, TC5013,
568 doi:10.1029/2006TC002081.
569 Vermeesch, P., 2007. CosmoCalc: An Excel add-in for cosmogenic nuclide calculations,
570 *Geochem. Geophys. Geosyst.,* **8**, Q08003, doi:10.1029/2006GC001530.

571 ***Appendix: Comparison of depth-profile concentrations with surface concentrations***
572
573 The comparison between surface concentrations and depth-profile concentrations
574 cannot be performed directly because cosmogenic nuclide production rate is extremely
575 sensitive to depth. Theoretically, concentrations only resulting from accumulation at any
576 depth below the surface (i.e., *in-situ* production with no denudation and no inheritance) may
577 be converted to concentrations the samples would have accumulated at the surface during the
578 same exposure duration using the inverse function of neutron attenuation. However,
579 concerning the analyzed Iranian sites, where scattering of both depth-profile and surface
580 concentrations is observed within alluvial material, this depth to surface conversion cannot be
581 achieved *a priori* because the measured concentrations are the result of two unknown
582 components: the *in-situ* exposure duration and the variable inheritance. Consequently, it is
583 only possible to perform an *a posteriori* comparison, which relies on the estimated
584 abandonment ages of an analyzed alluvial surface. For each abandonment age, the
585 corresponding *in-situ* contribution may be calculated for any depth-profile sample.
586 Subtracting this calculated *in-situ* contribution from the measured concentration yields the
587 current excess concentration of a given depth-profile sample. Then, adding this current excess
588 concentration to the *in-situ* concentration accumulated at the surface, during an exposure
589 duration corresponding to the abandonment age, yields to the concentration that the depth-
590 profile samples would have if emplaced and remaining at the surface. Performing such
591 concentration conversion for all the samples of a depth-profile allows comparing depth-
592 profile samples to surface samples.
593 Table A.1 provides all the measured cosmogenic nuclide concentrations and all the
594 results of the calculation that have been performed to convert depth-profile concentrations to
595 surface ones. For each analyzed site, these concentration conversions have been made at least
596 for two exposure durations: (1) the maximum abandonment age (t_{Max}), which has been
597 determined by the profile rejuvenation method (see section 2 and 3), and (2) the minimum
598 abandonment age (t_{min}), calculated from the lowest surface concentration. When OSL ages
599 were available, they have also been used to perform a depth to surface conversion. In
600 addition, a last column provides the inherited concentration at the time of alluvial aggradation
601 (i.e., the inheritance resulting form pre-exposure). It corresponds to the current excess
602 concentration corrected for radioactive decay.
603 Three figures illustrate the distribution of the measured surface concentrations and of
604 the differently converted depth-profile concentrations to surface ones. These figures are

presented in the same order as the sites analyzed in the text. Concerning the site of T2 terrace (see section 2), three abandonment ages are considered: 107 ka (t_{Max}), 50ka (t_{min}), and 30 ka (t_{OSL}). All the converted depth-profile concentrations, calculated using these abandonment ages are compared to the surface concentrations (Figure A.1 and Table A.1). This comparison indicates that the depth-profile and surface samples originate from the same source. Thus, they can be compared and analyzed jointly. Nevertheless, it appears that the converted depth-profile concentrations systematically exhibit a narrower range of values than the surface concentrations. This should be the consequence of the sampling amalgamation that tends to average the actual sample variability. The converted depth-profile concentrations decrease with the abandonment ages. Nevertheless, while the *in-situ* contribution decreases with the abandonment age, inheritance remains comparable within the range ≈3 to $8.5x10^5$ at/g. For the T3 site (section 3.1), only two abandonment ages may be considered. All the converted depth-profile concentrations, calculated using both cosmogenic nuclide abandonment ages are compared to the measured surface concentrations (Figure A.2 and Table A.1). However, the two abandonment cosmogenic nuclide ages yield significant differences as the two possible ranges of converted concentrations do not nearly overlap. The depth-profile concentrations converted using 412 ka (t_{Max}) are within the range of the measured surface concentrations that defines the Gaussian distribution (see figure 4a, right) while those converted using 235 ka (t_{min}) lie between the Gaussian distribution of the measured surface concentrations and the measured lowest surface concentration. Depending on whether the lowest surface concentration is interpreted as the best t_{min} approximation or as an outlier, this solution may be considered as valid or not. Whatever the choice, as mentioned in section 3.1, the solution based on 412 ka provides a significantly higher value for the maximum inheritance than the mean determined by profile modelling (see Figure 4b and Table A.1). Concerning the T1 terrace site (see section 3.2), three abandonment ages are considered: 46 ka (t_{Max}), 17.5 ka (t_{min}), and 10 ka (t_{OSL}). All but the one based on 46 ka of the converted depth-profile concentrations are within the range of the surface concentrations (Figure A.3 and Table A.1). However, it is noteworthy to stress that the results obtained considering t_{Max} are inconsistent with the T1 surface data. Then, this maximum cosmogenic nuclide abandonment age is most likely unrealistic. Considering the two younger abandonment ages of 17.5 ka and 10 ka, the obtained converted concentrations are compared with the measured surface concentrations (Figure A.3). As for the T2 site, they appear to determine a narrower range of values than the surface concentrations. At this site, the range of inheritance, from ~1.5 to $4.5x10^5$ at/g, also remains approximately stable even if the abandonment age decreases.

639 Therefore, the comparison between the depth-profile and the surface concentrations,
640 which can be realized *a posteriori*, indicates that all the alluvial samples originate from the
641 same variably pre-exposed source. As a consequence, depth-profile and surface samples can
642 be analyzed jointly.

643
644 ***Figure captions***
645
646 Figure 1: Usual strategies of surface and depth-profile sampling for determining exposure age
647 of alluvial surfaces. a) Individual quartz pebbles are collected for surface sampling while
648 amalgams of 10-30 centimetre-sized pebbles are used for depth-profile sampling. b) Surface
649 exposure age determination using (top) weighted mean ^{10}Be CRE age for surface samples and
650 (bottom) modelling an exponential decrease of the concentrations with depth for depth-profile
651 samples. Blue and black samples for theoretical cases, dark pink and light pink domains
652 figure out the *in-situ* production acquired with and without homogeneous inheritance,
653 respectively. With homogeneous inheritance, the Gaussian distribution of the surface samples
654 is shifted providing an artificial CRE age older than the current age of surface abandonment.
655 The shift corresponds to the inherited ^{10}Be concentration that the modelling of a depth-profile
656 may evidence. The homogeneous inheritance is the concentration value toward which the
657 modelled profile asymptotically tends. c) With a variable inheritance, CRE surface ages are
658 often scattered and their distribution is multimodal. There is no exponential decrease of the
659 concentrations with depth making helpless any profile modelling (dashed curve).
660
661 Figure 2 : Illustration of the rejuvenation method. a) Red dots are the concentrations measured
662 for the depth-profile amalgams and the surface samples. If there is no denudation, then the
663 scatter of concentrations results only from a variable inheritance. b) The first step requires
664 calculating the time needed for one of the depth-profile samples to be brought back to a null
665 concentration without bringing the other samples to a negative concentration. The
666 concentration of that sample is indicated in red while the theoretical *in-situ* concentration
667 expected at the depth of the other profile samples is indicated by blue dots. The *in-situ*
668 exposure duration required to bring that depth-profile sample to its measured concentration
669 corresponds to the maximum abandonment age (t_{Max}) of the terrace and is indicated in red
670 with the pink domain figuring the corresponding *in-situ* production. The blue arrows indicate
671 the excess concentrations remaining in the other depth-profile samples. c) The second step
672 consists in comparing these rejuvenated profile concentrations with the rejuvenated surface
673 samples (blue dots with error bars). If the profile rejuvenation shifts most of the surface
674 concentrations to positive values (left panel), then the calculated abandonment age provides a
675 maximum possible age for the surface. On the other hand, if most of the rejuvenated surface
676 concentrations are shifted to negative values (right panel), there is inconsistency and the

677 calculated abandonment age overestimates the actual age of the surface. d) A third step allows
678 calculating a minimum abandonment age (t_{min}). Green dots are the concentrations obtained for
679 the depth-profile amalgams and for the surface samples once rejuvenated by the age of *in-situ*
680 exposure of the youngest surface sample at their sampling depth, assuming this youngest
681 sample on the surface best approximates its age of abandonment.
682
683 Figure 3: a) Inset is a simplified tectonic map of central and eastern Iran with major active
684 faults indicated. Black dot indicates site of sampling. On the right, surface age distribution of
685 the alluvial terrace T2 at the Dehshir South site. Weighted mean ^{10}Be CRE ages of the terrace
686 tread samples are indicated in red and in blue for the rejuvenated surface samples (for t_{Max},
687 see b). The thin curves represent the CRE age probability as Gaussian distribution for each
688 individual sample and the thick curves correspond to the summed Gaussian density
689 probability function. The uncertainties associated to the weighted mean age correspond to two
690 standard deviations (2σ). b) ^{10}Be depth-profile concentrations through the alluvial terrace.
691 Red dots are the concentrations measured in the depth-profile amalgams and in the surface
692 samples. Blue dots are the concentrations obtained for the depth-profile amalgams and the
693 surface samples once one depth-profile amalgam (P127) is restored to a null concentration
694 without bringing back any other depth-profile sample to a negative concentration. The time
695 (t_{Max}) of *in-situ* exposure to bring that depth-profile sample to its measured concentration is
696 indicated in red with the pink domain figuring the corresponding *in-situ* production. The blue
697 arrows indicate the excess concentrations remaining in the other depth-profile samples. c)
698 Green dots are the concentrations obtained for the depth-profile amalgams and for the surface
699 samples once rejuvenated by 50 ka of *in-situ* exposure (t_{min})at their sampling depth, assuming
700 the youngest sample on the surface best approximates its abandonment age. Weighted mean
701 ^{10}Be CRE ages of the terrace tread samples are indicated in red and in green once rejuvenated.
702
703 Figure 4: a) Inset is a simplified tectonic map of central and eastern Iran with major active
704 faults indicated. Black dot indicates site of sampling. On the right, surface age distribution of
705 the alluvial terrace T3 at the Dehshir North site. Weighted mean ^{10}Be CRE ages of the terrace
706 tread samples are indicated in red and in blue for the rejuvenated surface samples (for t_{Max},
707 see b). The thin curves represent the CRE age probability as Gaussian distribution for each
708 individual sample and the thick curves correspond to the summed Gaussian density
709 probability function. The uncertainties associated to the weighted mean age correspond to two
710 standard deviations (2σ). b) ^{10}Be depth-profile concentrations through the alluvial terrace.

Red dots are the concentrations measured for the depth-profile amalgams and the surface samples. Blue dots are the concentrations obtained for the depth-profile amalgams and the surface samples once one depth-profile amalgam (P12) is restored to a null concentration without bringing back any other depth-profile sample to a negative concentration. The time (t_{Max}) of *in-situ* exposure to bring that depth-profile sample to its measured concentration is indicated in red with the pink domain figuring the corresponding *in-situ* production. The blue arrows indicate the excess concentrations remaining in the other depth-profile samples. The curve showing the best fit to the depth-profile concentrations is obtained with an age of 464 ka, a homogeneous inheritance of 3.8×10^5 at/g (SiO_2), a null denudation rate and a χ^2 of 931. c) Green dots are the concentrations obtained for the depth-profile amalgams and for the surface samples once rejuvenated by 235 ka of *in-situ* exposure duration (t_{min}) at their sampling depth, assuming the youngest sample on the surface best approximates its age of abandonment. Weighted mean ^{10}Be CRE ages of the terrace tread samples are indicated in red and in green once rejuvenated.

Figure 5: a) Inset is a simplified tectonic map of central and eastern Iran with major active faults indicated. Black dot indicates site of sampling. On the right, surface age distribution of the alluvial terrace T1 at the Anar site. Weighted mean ^{10}Be CRE ages of the terrace tread samples are indicated in red and in blue for the rejuvenated surface samples (for t_{Max}, see b). The thin curves represent the CRE age probability as Gaussian distribution for each individual sample and the thick curves correspond to the summed Gaussian density probability function. The uncertainties associated to the weighted mean age correspond to two standard deviations (2σ). b) ^{10}Be depth-profile concentrations through the alluvial terrace. Red dots are the measured concentrations of the depth-profile amalgams and surface samples. Blue dots are the concentrations obtained for the depth-profile amalgams and surface samples once one depth-profile amalgam (P102) is restored to a null concentration without bringing back any other depth-profile sample to a negative concentration. The time (t_{Max}) of *in-situ* exposure to bring that depth-profile sample to its measured concentration is indicated in red with the pink domain figuring the corresponding *in-situ* production. The blue arrows indicate the excess concentrations remaining in the other depth-profile samples. Note that only one of the rejuvenated surface samples would display a positive concentration (see text for discussion). c) Green dots are the concentrations obtained for the depth-profile amalgams and for the surface samples once rejuvenated by 17.5 ka of *in-situ* exposure duration (t_{min}) at their sampling depth, assuming the youngest sample on the surface best approximates its age of

abandonment.

Figure A.1: a) Distribution of surface ^{10}Be measured concentration for alluvial terrace T2. ^{10}Be depth-profile concentrations converted to the surface for abandonment ages of 107 ka (b), 50 ka (c), and 30 ka (d), respectively (see text of appendix). For each graph the thin coloured curves represent the concentrations probability as Gaussian distribution for each individual sample and the thick black curves correspond to the summed Gaussian density probability function.

Figure A.2: a) Distribution of surface ^{10}Be measured concentration for alluvial terrace T3. ^{10}Be depth-profile concentrations converted to the surface for abandonment ages of 412 ka (b) and 235 ka (c), respectively (see text of appendix). For each graph the thin coloured curves represent the concentrations probability as Gaussian distribution for each individual sample and the thick black curves correspond to the summed Gaussian density probability function.

Figure A.3: a) Distribution of surface ^{10}Be measured concentration for alluvial terrace T1. ^{10}Be depth-profile concentrations converted to the surface for abandonment ages of 46 ka (b), 17.5 ka (c), and 10 ka (d), respectively (see text of appendix). For each graph the thin coloured curves represent the concentrations probability as Gaussian distribution for each individual sample and the thick black curves correspond to the summed Gaussian density probability function.

Table 1: The ^{10}Be concentrations and CRE modelled ages for surface and depth-profile samples along the Dehshir and Anar fault. Propagated analytical uncertainties (reported as 1σ) include uncertainties associated with AMS counting statistics, chemical blank measurements and AMS internal error (0.5%). Zero erosion zero inheritance model ages are calculated for surface samples taking into account their associated analytical uncertainties, their sampling geographic coordinates and no shielding, in agreement with site topography. The used ^{10}Be half-life is 1.387 Ma (Chmeleff et al., 2010; Korschinek et al., 2010). For surface samples, a density of 2.2 g.cm^{-3} has been used for quartz. An attenuation length of 160 g.cm^{-2} (Gosse & Philipps, 2001) has been used for fast neutrons. Stone (2000) polynomial has been used to determine surface production rate at the sampling geographic coordinates assuming a SLHL production rate of 4.49 at.g^{-1}.yr^{-1} for ^{10}Be with 6% of uncertainty. ^{10}Be ages have been calculated using Cosmocalc (Vermeesh 2007). About 10-30 pebbles with centimetre size have been generally collected for the amalgamated samples of the profiles. Anar samples ages

781 differ slightly from those published in Le Dortz et al. (2009) because they have been
782 recalculated with updated half-life and attenuation length.
783
784
785 Table A.1: The table presents the measured and calculated parameters used to compare depth-
786 profile and surface concentrations for different abandonment ages (t_{Max} obtained from the
787 profile rejuvenation method, t_{min}, obtained from the youngest surface pebble and t_{OSL} when
788 OSL ages are available) of each analyzed alluvial terrace, T2, T3, and T1. The excess
789 concentrations correspond to the concentrations remaining in depth-profile samples after
790 using the rejuvenation method. For each depth-profile sample, adding up this excess
791 concentration to the concentration corresponding to the *in-situ* surface duration (t_{Max}; t_{min} or
792 t_{OSL}) permit to calculate the profile ^{10}Be concentration converted to the surface for each
793 abandonment age. This concentration would correspond for each depth-profile sample to their
794 concentration if they had emplaced and remained at the surface ; it can be compared to the
795 concentrations measured in the surface samples. Correcting the excess concentration for
796 radioactive decay allows calculating the ^{10}Be inheritance in each depth-profile sample, which
797 corresponds to the inheritance value at the time of the alluvial aggradation.
798

Highlights

- Surface and depth profile cosmogenic sampling
- If scattering of concentrations (profile & surface), there is variable inheritance
- If erosion is negligible, we use profile rejuvenation method
- Minimum inheritance, hence, maximum abandonment age for the surface is obtained

Samples	Sample description	Density ($g.cm^{-3}$)	Thickness (cm)	Latitude (°N)	Longitude (°E)	Elevation (m)	Stone scaling factor	Measured ^{10}Be (10^5 at.$g^{-1}SiO2$)	zero inheritance zero erosion ^{10}Be model age (ka)
Terrace T2 (Dehshir South)									
Surface sampling									
DS06S32	cobble (10 cm)	2.2	5	30.4476	54.12655	1622	2.78	21.01±0.52	175.57±11.39
DS06S34	cobble (20 cm)	2.2	6	30.44765	54.12751	1619	2.77	21.95±0.32	184.19±11.38
DS06S36	cobble (20 cm)	2.2	6	30.447	54.1284	1620	2.77	15.08±0.24	124.58±7.73
DS08S111	cobble (10 cm)	2.2	6	30.44792	54.13517	1612	2.76	18.52±0.49	154.99±10.15
DS08S112	cobble (10 cm)	2.2	7	30.44793	54.13371	1615	2.76	22.12±0.60	186.22±12.26
DS08S113	cobble (10 cm)	2.2	7	30.44708	54.13213	1618	2.77	26.61±0.68	225.76±14.73
DS08S114	cobble (10 cm)	2.2	6	30.44803	54.13074	1623	2.78	6.16±0.17	49.87±3.29
Profile sampling						1645			
DS08P126	amalgam 30 cm below ground surface	2.2	-	30.44823	54.12648		2.82	11.23±0.30	
DS08P127	amalgam 60 cm below ground surface	2.2	-	30.44823	54.12648		2.82	6.10±0.17	
DS08P128	amalgam 100 cm below ground surface	2.2	-	30.44823	54.12648		2.82	5.82±0.16	
DS08P129	amalgam 150 cm below ground surface	2.2	-	30.44823	54.12648		2.82	5.91±0.16	
DS08P130	amalgam 210 cm below ground surface	2.2	-	30.44823	54.12648		2.82	8.86±0.24	
DS08P131	amalgam 270 cm below ground surface	2.2	-	30.44823	54.12648		2.82	3.62±0.10	
DS08P132	amalgam 370 cm below ground surface	2.2	-	30.44823	54.12648		2.82	4.31±0.12	
Terrace T3 (Dehshir North)									
Surface sampling									
DN06S2	2 fragments of the same gelyfracted cobble	2.2	3	30.64065	54.01907	1550	2.66	26.55±3.66	235.55±35.38
DN06S6	cobble (10 cm)	2.2	5	30.64036	54.021083	1550	2.66	51.88±0.72	489.51±30.15
DN06S7	cobble (15 cm)	2.2	4	30.64045	54.02092	1550	2.66	48.78±1.19	456.66±29.58
DN06S10	cobble (10 cm)	2.2	5	30.6405	54.020917	1550	2.66	49.21±0.69	461.15±28.42
DN06A11	Amalgam (20 pluricentimetric clasts)	2.2	-	30.6405	54.020917	1550	2.66	48.37±0.66	452.25±27.83
DN06S19	cobble (10 cm)	2.2	4	30.64208	54.02502	1550	2.66	46.84±0.65	436.33±26.88
DN06S21	cobble (10 cm)	2.2	4	30.64189	54.02503	1550	2.66	54.60±0.75	518.71±31.93
DN06S23	cobble (10 cm)	2.2	7	30.64177	54.0251	1550	2.66	50.72±2.12	477.09±34.88
DN06S26	cobble (10 cm)	2.2	8	30.64101	54.02506	1550	2.66	46.99±1.02	437.88±27.94
DN06S28	cobble (20 cm)	2.2	9	30.64038	54.02512	1550	2.66	45.92±0.99	426.74±27.23
Profile sampling						1550			
DN06P12Q	amalgam 25 cm below ground surface	2.2	-	30.64114	54.02133		2.66	33.77±0.85	
DN06P13Q	amalgam 55 cm below ground surface	2.2	-	30.64114	54.02133		2.66	25.80±0.66	
DN06P14Q	amalgam 95 cm below ground surface	2.2	-	30.64114	54.02133		2.66	22.12±0.45	
DN06P15Q	amalgam 165 cm below ground surface	2.2	-	30.64114	54.02133		2.66	13.60±0.34	
DN06P16Q	amalgam 230 cm below ground surface	2.2	-	30.64114	54.02133		2.66	6.89±0.17	
DN06P17Q	amalgam 270 cm below ground surface	2.2	-	30.64114	54.02133		2.66	4.37±0.07	
DN06P18Q	amalgam 305 cm below ground surface	2.2	-	30.64114	54.02133		2.66	9.68±0.24	

Terrace T1 (Anar)

Surface sampling									
AS06S73	Amalgam - pluricentimetric fragment	2.2	-	31.19474	55.15243	1574	2.73	7.86 ± 0.18	64.27 ± 4.12
AS06S74	Amalgam - pluricentimetric fragment	2.2	-	31.19404	55.15357	1562	2.71	3.93 ± 0.12	31.86 ± 2.16
AS06S75	3 fragments of the same gelyfracted pebble	2.2	4	31.19263	55.15304	1571	2.73	2.20 ± 0.05	17.45 ± 1.12
AS06S76	conglomerate with pebbles of quartz (cm)	2.2	9	31.19405	55.15330	1559	2.71	2.55 ± 0.06	20.34 ± 1.30
AS08S89	fragment of a cobble	2.2	5	31.20095	55.15331	1571	2.73	3.53 ± 0.086	28.90 ± 1.87
AS08S91	several fragments of the same gelyfracted pebble	2.2	-	31.19915	55.15242	1571	2.73	3.47 ± 0.08	28.40 ± 1.84
AS08S92	Amalgam - pluricentimetric fragment	2.2	-	31.19874	55.15221	1570	2.73	3.96 ± 0.10	32.50 ± 2.11
AS08S94	two fragments of the same gelyfracted pebble	2.2	6	31.19391	55.15297	1570	2.73	5.20 ± 0.12	42.74 ± 2.77
AS08S95	pebble (10 cm)	2.2	6	31.19499	55.15471	1570	2.73	2.70 ± 0.067	22.06 ± 1.43
AS08S96	pebble (10 cm)	2.2	5	31.19358	55.15577	1570	2.73	3.83 ± 0.10	31.45 ± 2.08
Profile sampling						1567			
AS08P97	amalgam 370 cm below ground surface	2.2	-	31.19526	55.15340		2.72	4.29 ± 0.12	
AS08P98	amalgam 270 cm below ground surface	2.2	-	31.19527	55.15341		2.72	3.48 ± 0.09	
AS08P99	amalgam 170 cm below ground surface	2.2	-	31.19527	55.15341		2.72	4.21 ± 0.11	
AS08P100	amalgam 100 cm below ground surface	2.2	-	31.19527	55.15341		2.72	2.24 ± 0.06	
AS08P101	amalgam 70 cm below ground surface	2.2	-	31.19527	55.15341		2.72	5.15 ± 0.14	
AS08P102	amalgam 30 cm below ground surface	2.2	-	31.19527	55.15341		2.72	3.8 ± 0.10	
AS08P108	amalgam 150 cm below ground surface	2.2	-	31.19527	55.15341		2.72	1.8 ± 0.05	

T2

T2 Surface

Samples	Depth (cm)	Measured ^{10}Be (10^5 at.g^{-1}SiO$_2$)
DS06S32	0	21.01±0.52
DS06S34	0	21.95±0.32
DS06S36	0	15.08±0.24
DS08S111	0	18.52±0.49
DS08S112	0	22.12±0.60
DS08S113	0	26.61±0.68
DS08S114	0	6.16±0.17

T2 Depth profile

Abandonment age	Samples	Depth (cm)	Abandonment age	Excess concentration (10^5 at.g^{-1} SiO$_2$)	^{10}Be inheritance (10^5 at.g^{-1} SiO$_2$)	Profile ^{10}Be concentration converted to surface (10^5 at.g^{-1} SiO$_2$)
DS08P126	30	11.23±0.30		2.15±0.06	2.27±0.06	15.74±0.42
DS08P127	60	6.10±0.17		0	0	13.59±0.37
DS08P128	100	5.82±0.16		2.18±0.06	2.30±0.06	15.77±0.44
DS08P129	150	5.91±0.16	107 ka	3.96±0.11	4.17±0.12	17.54±0.48
DS08P130	210	8.86±0.24		7.86±0.21	8.29±0.22	21.45±0.57
DS08P131	270	3.62±0.10		3.05±0.08	3.22±0.09	16.64±0.47
DS08P132	370	4.31±0.12		4.00±0.11	4.22±0.12	17.59±0.48
DS08P126	30	11.23±0.30		6.92±0.19	7.10±0.19	13.09±0.35
DS08P127	60	6.10±0.17		3.21±0.09	3.29±0.09	9.37±0.25
DS08P128	100	5.82±0.16		4.09±0.11	4.19±0.12	10.25±0.30
DS08P129	150	5.91±0.16	50 ka	8.38±0.13	5.11±0.14	11.15±0.31
DS08P130	210	8.86±0.24		3.35±0.26	8.59±0.23	14.54±0.39
DS08P131	270	3.62±0.10		4.16±0.09	3.44±0.09	9.51±0.27
DS08P132	370	4.31±0.12		4.16±0.12	4.27±0.12	10.32±0.28
DS08P126	30	11.23±0.30		8.63±0.23	8.76±0.23	12.44±0.33
DS08P127	60	6.10±0.17		4.36±0.12	4.42±0.12	8.17±0.22
DS08P128	100	5.82±0.16		4.78±0.13	4.85±0.14	8.59±0.24
DS08P129	150	5.91±0.16	30 ka	5.35±0.14	5.43±0.15	9.16±0.25
DS08P130	210	8.86±0.24		8.57±0.23	8.70±0.23	12.38±0.31
DS08P131	270	3.62±0.10		3.46±0.09	3.51±0.10	7.27±0.21
DS08P132	370	4.31±0.12		4.21±0.12	4.28±0.12	8.03±0.22

T3

T3 Surface

Samples	Depth (cm)	Measured ^{10}Be (10^5 at.g^{1} SiO$_2$)
DN06S2	0	26.55±3.66
DN06S6	0	51.88±0.72
DN06S7	0	48.78±1.19
DN06S10	0	49.21±0.69
DN06A11	0	48.37±0.66
DN06S19	0	46.84±0.65
DN06S21	0	54.60±0.75
DN06S23	0	50.72±2.12
DN06S26	0	46.99±1.02
DN06S28	0	45.92±0.99

T3 Depth profile

Samples	Depth (cm)	Measured ^{10}Be (10^5 at.g^{-1} SiO$_2$)	Abandonment age	Excess concentration (10^5 at.g^{-1} SiO$_2$)	^{10}Be inheritance (10^5 at.g^{-1} SiO$_2$)	Profile ^{10}Be concentration converted to surface (10^5 at.g^{-1} SiO$_2$)
DN06P12Q	25	33.77±0.85	412 ka	0	0	45.53±1.15
DN06P13Q	55	25.80±0.66		3.84±0.09	4.71±0.12	49.36±1.25

DN06P14Q	95	22.12±0.45		9.04±0.18	11.10±0.22	54.56±1.10
DN06P15Q	165	13.60±0.34		8.04±0.20	9.88±0.24	53.57±1.33
DN06P16Q	230	6.89±0.17		4.12±0.10	5.06±0.13	49.65±1.25
DN06P17Q	270	4.37±0.07		2.43±0.04	2.99±0.05	47.96±0.77
DN06P18Q	305	9.68±0.24		8.18±0.20	10.06±0.25	53.71±1.33
DN06P12Q	25	33.77±0.85		13.68±0.34	15.38±0.39	40.28±1.01
DN06P13Q	55	25.80±0.66		12.73±0.33	14.32±0.36	39.33±1.00
DN06P14Q	95	22.12±0.45		14.33±0.29	16.12±0.33	40.93±0.83
DN06P15Q	165	13.60±0.34	235 ka	10.29±0.25	11.57±0.29	36.89±0.91
DN06P16Q	230	6.89±0.17		5.24±0.13	5.89±0.15	31.84±0.80
DN06P17Q	270	4.37±0.07		3.22±0.05	3.62±0.06	29.82±0.48
DN06P18Q	305	9.68±0.24		8.79±0.22	9.89±0.24	35.39±0.87

T1

T1 Surface

Samples	**Depth (cm)**	**Measured ^{10}Be (10^5 at.g^{-1} SiO_2)**
AS06S73	0	7.86 ± 0.18
AS06S74	0	3.93 ± 0.12
AS06S75	0	2.20 ± 0.05
AS06S76	0	2.55 ± 0.06
AS08S89	0	3.53 ± 0.086
AS08S91	0	3.47 ± 0.08
AS08S92	0	3.96 ± 0.10
AS08S94	0	5.20 ± 0.12
AS08S95	0	2.70 ± 0.067
AS08S96	0	3.83 ± 0.10

T1 Depth profile

Samples	**Depth (cm)**	**Measured ^{10}Be (10^5 at.g^{-1} SiO_2)**	**Abandonment age**	**Excess concentration (10^5 at.g^{-1} SiO_2)**	**^{10}Be inheritance (10^5 at.g^{-1} SiO_2)**	**Profile ^{10}Be concentration converted to surface (10^5 at.g^{-1} SiO_2)**
AS08P97	370	4.29 ± 0.12		4.16±0.11	4.26±0.12	9.80±0.27
AS08P98	270	3.48 ± 0.09		3.24±0.09	3.32±0.09	8.88±0.24
AS08P99	170	4.21 ± 0.11		3.55±0.09	3.64±0.10	9.19±0.25
AS08P100	100	2.24 ± 0.06	46 ka	0.70±0.02	0.72±0.02	6.34±0.17
AS08P101	70	5.15 ± 0.14		2.89±0.08	2.96±0.08	8.53±0.23
AS08P102	30	3.8 ± 0.10		0	0	5.64±0.15
AS08P108	150	1.8 ± 0.05		0.97±0.03	0.99±0.03	6.61±0.19
AS08P97	370	4.29 ± 0.12		4.24±0.12	4.28±0.12	6.44±0.17
AS08P98	270	3.48 ± 0.09		3.39±0.09	3.42±0.09	5.59±0.15
AS08P99	170	4.21 ± 0.11		3.95±0.11	3.99±0.11	6.15±0.17
AS08P100	100	2.24 ± 0.06	17.5 ka	1.63±0.04	1.65±0.05	3.83±0.11
AS08P101	70	5.15 ± 0.14		4.26±0.12	4.30±0.12	6.46±0.17
AS08P102	30	3.8 ± 0.10		2.29±0.06	2.31±0.06	4.49±0.12
AS08P108	150	1.8 ± 0.05		1.47±0.04	1.48±0.04	3.67±0.10
AS08P97	370	4.29 ± 0.12		4.26±0.12	4.29±0.12	5.49±0.15
AS08P98	270	3.48 ± 0.09		3.43±0.09	3.45±0.09	4.66±0.13
AS08P99	170	4.21 ± 0.11		5.07±0.11	4.09±0.11	5.30±0.14
AS08P100	100	2.24 ± 0.06	10 ka	1.90±0.05	1.91±0.05	3.13±0.08
AS08P101	70	5.15 ± 0.14		4.65±0.13	4.68±0.12	5.88±0.16
AS08P102	30	3.8 ± 0.10		2.96±0.08	2.97±0.08	4.18±0.11
AS08P108	150	1.8 ± 0.05		1.61±0.05	1.62±0.05	2.28±0.08

Figure 1

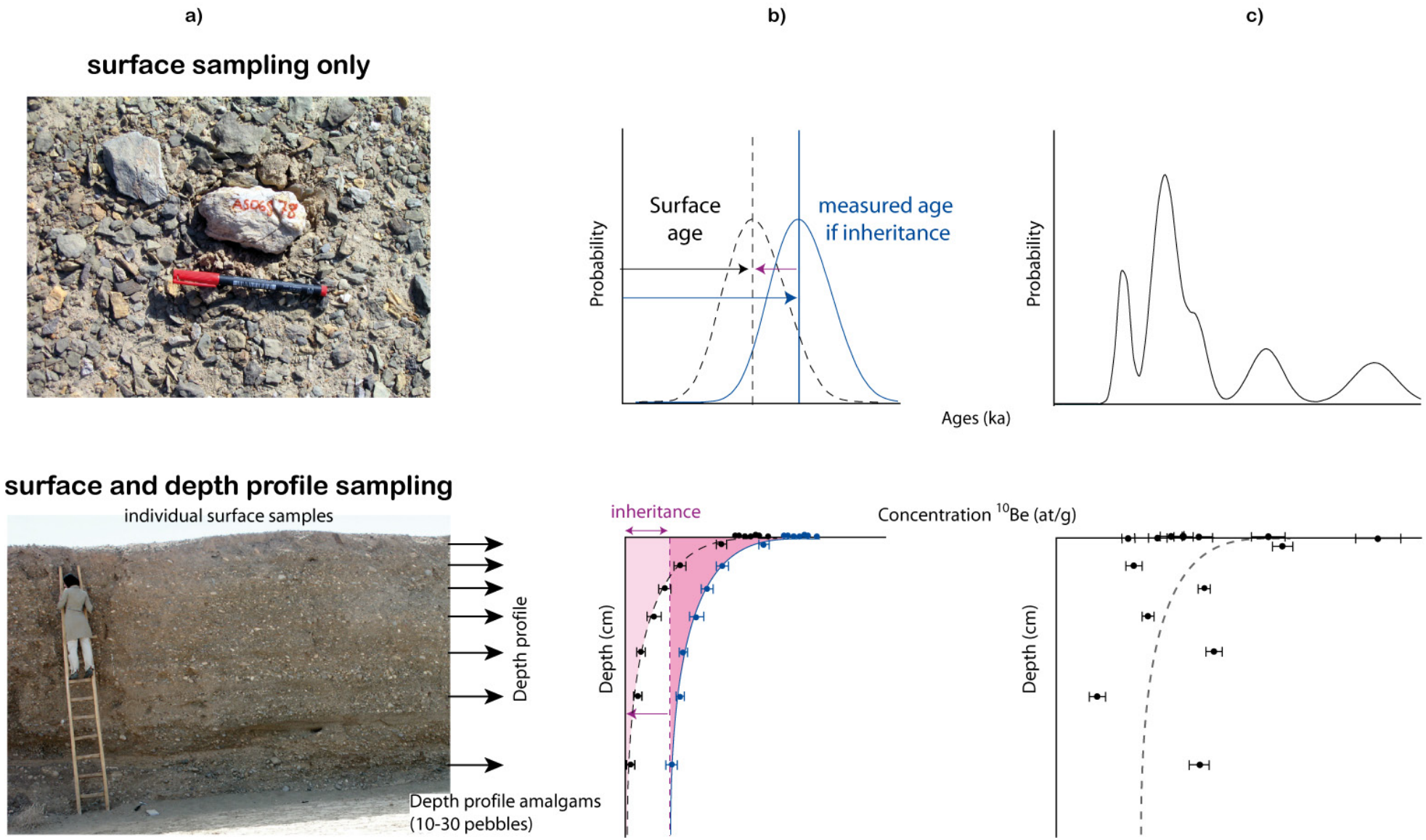
a)
b)
c)
surface sampling only
Surface age
measured age if inheritance
Probability
Ages (ka)
Probability
surface and depth profile sampling
individual surface samples
Depth profile
Depth profile amalgams (10-30 pebbles)
inheritance
Depth (cm)
Concentration ^{10}Be (at/g)
Depth (cm)

Figure 2

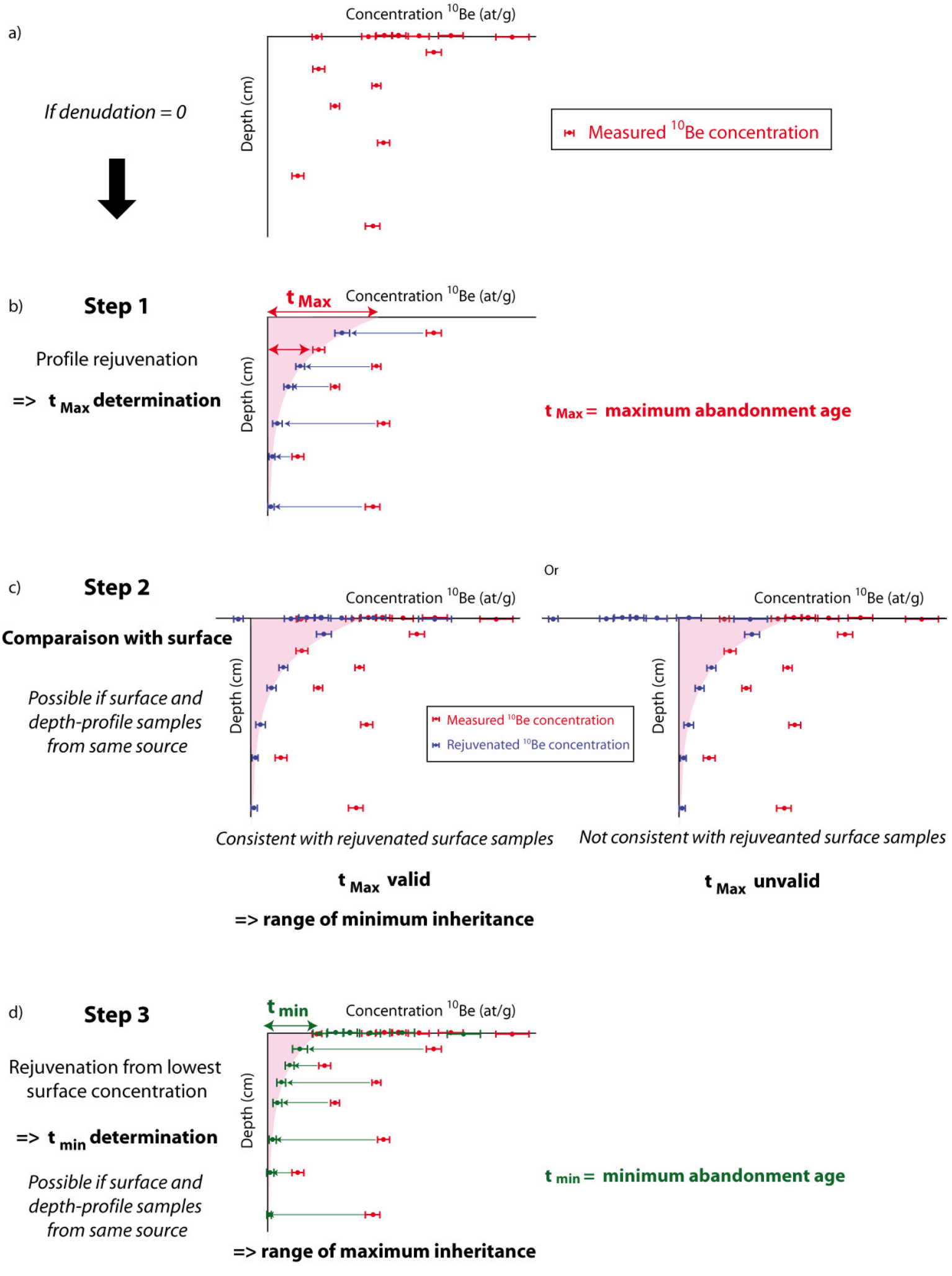
a)
If denudation = 0
Concentration ^{10}Be (at/g)
Depth (cm)
Measured ^{10}Be concentration
b)
Step 1
Profile rejuvenation
=> t_{Max} determination
t_{Max}
Concentration ^{10}Be (at/g)
Depth (cm)
t_{Max} = maximum abandonment age
c)
Step 2
Comparaison with surface
Possible if surface and depth-profile samples from same source
Concentration ^{10}Be (at/g)
Depth (cm)
Measured ^{10}Be concentration
Rejuvenated ^{10}Be concentration
Consistent with rejuvenated surface samples
t_{Max} valid
=> range of minimum inheritance
Or
Concentration ^{10}Be (at/g)
Depth (cm)
Not consistent with rejuveanted surface samples
t_{Max} unvalid
d)
Step 3
Rejuvenation from lowest surface concentration
=> t_{min} determination
Possible if surface and depth-profile samples from same source
t_{min}
Concentration ^{10}Be (at/g)
Depth (cm)
t_{min} = minimum abandonment age
=> range of maximum inheritance

Figure 3

a)

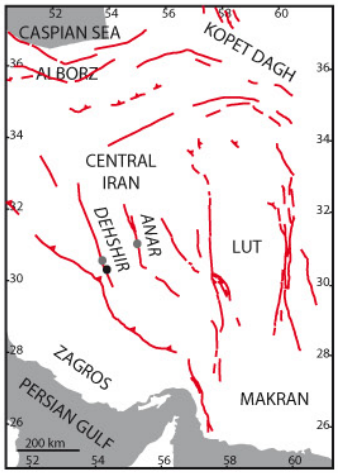
CASPIAN SEA
KOPET DAGH
ALBORZ
CENTRAL IRAN
DEHSHIR
ANAR
LUT
ZAGROS
PERSIAN GULF
MAKRAN
200 km

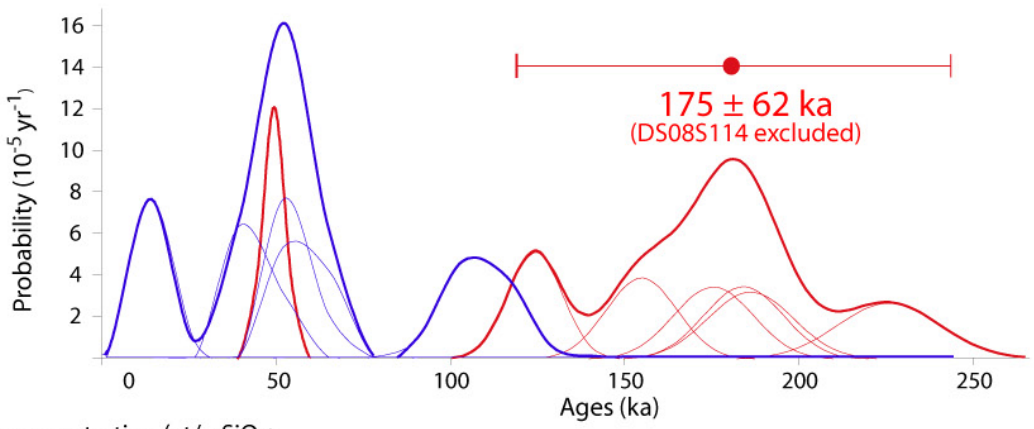
Terrace T2
175 ± 62 ka
(DS08S114 excluded)
Probability (10^{-5} yr^{-1})
Ages (ka)

b)

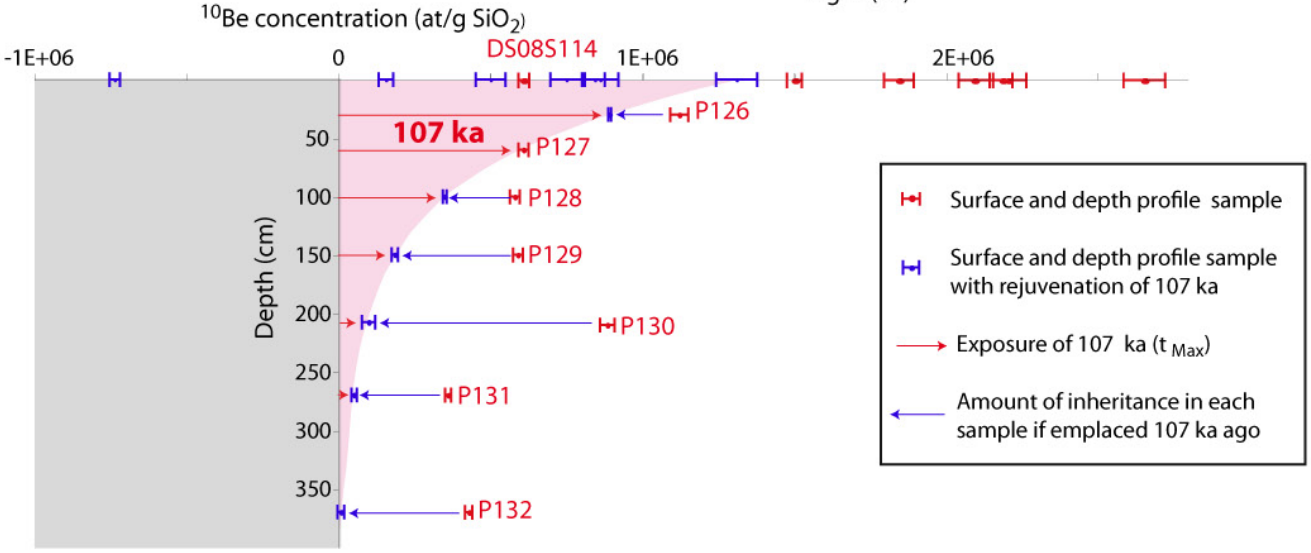
^{10}Be concentration (at/g SiO$_2$)
DS08S114
107 ka
P126
P127
P128
P129
P130
P131
P132
Depth (cm)
Surface and depth profile sample
Surface and depth profile sample with rejuvenation of 107 ka
Exposure of 107 ka (t Max)
Amount of inheritance in each sample if emplaced 107 ka ago

c)

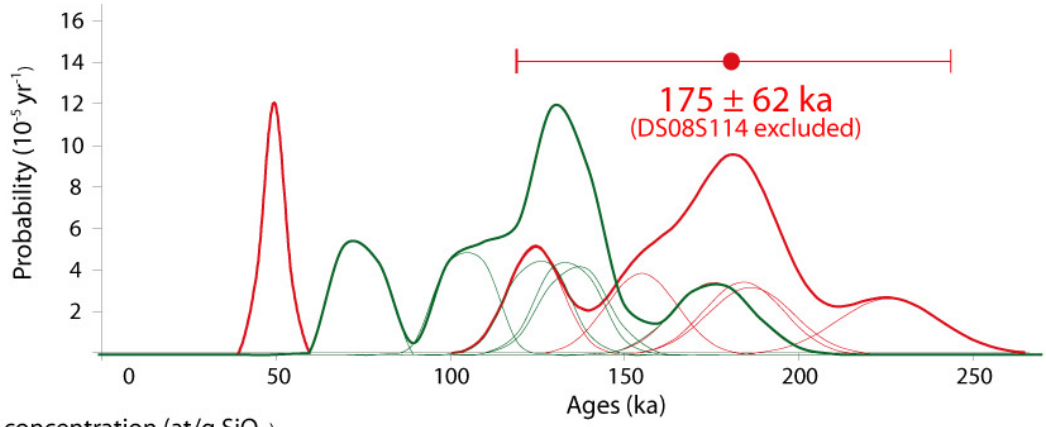
175 ± 62 ka
(DS08S114 excluded)
Probability (10^{-5} yr^{-1})
Ages (ka)

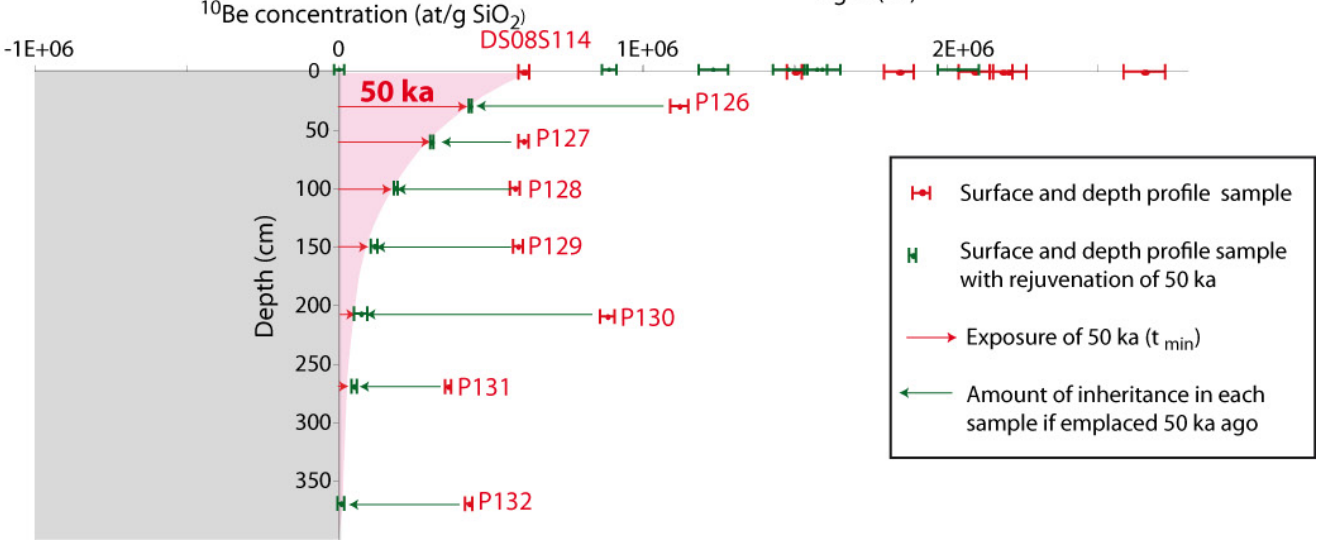
^{10}Be concentration (at/g SiO$_2$)
DS08S114
50 ka
P126
P127
P128
P129
P130
P131
P132
Depth (cm)
Surface and depth profile sample
Surface and depth profile sample with rejuvenation of 50 ka
Exposure of 50 ka (t min)
Amount of inheritance in each sample if emplaced 50 ka ago

Figure 4

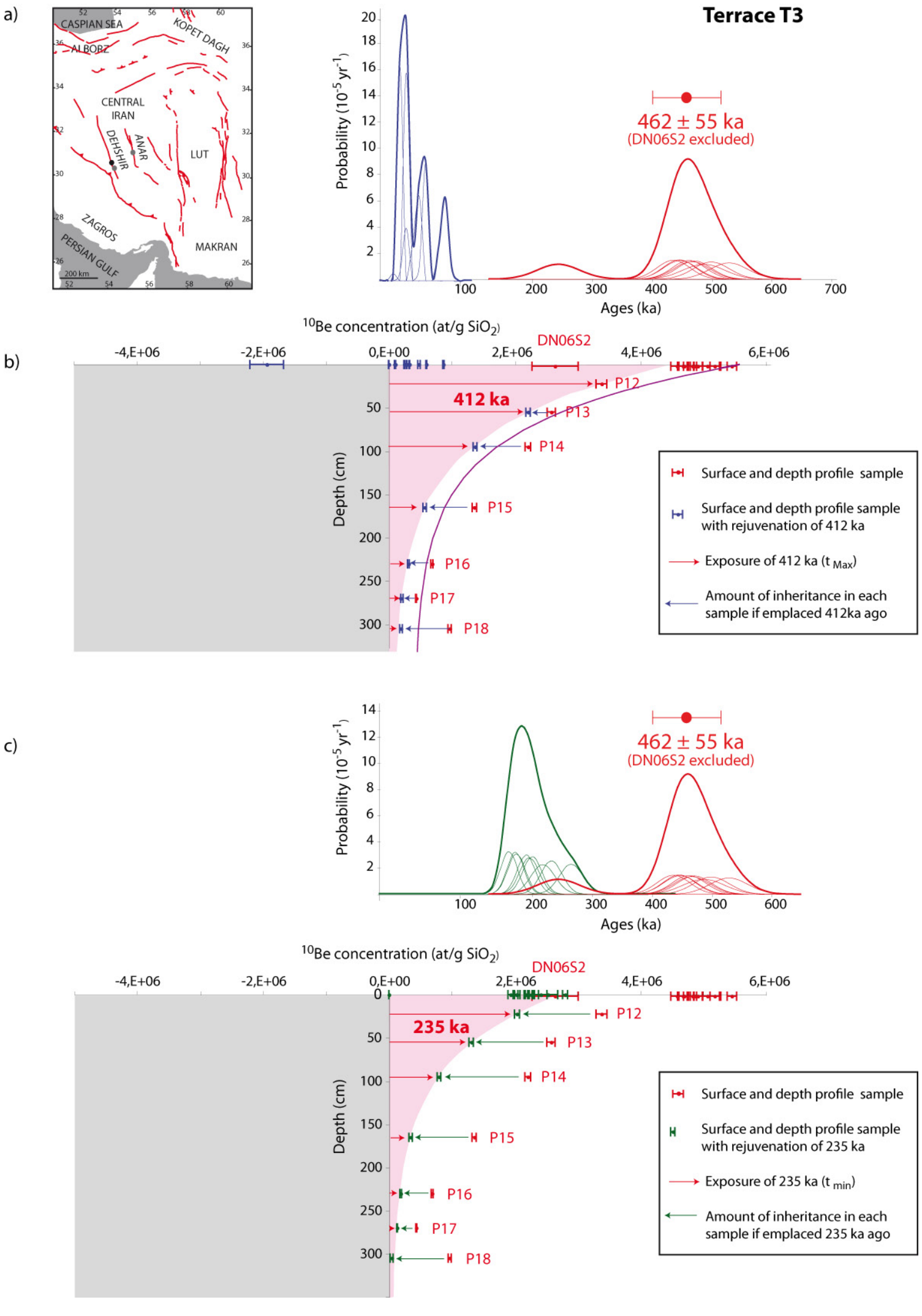
a)
CASPIAN SEA
KOPET DAGH
ALBORZ
CENTRAL IRAN
DEHSHIR
ANAR
LUT
ZAGROS
PERSIAN GULF
MAKRAN
200 km
Terrace T3
Probability (10^{-5} yr^{-1})
462 ± 55 ka
(DN06S2 excluded)
Ages (ka)
b)
^{10}Be concentration (at/g SiO$_2$)
DN06S2
412 ka
P12
P13
P14
P15
P16
P17
P18
Depth (cm)
Surface and depth profile sample
Surface and depth profile sample with rejuvenation of 412 ka
Exposure of 412 ka (t Max)
Amount of inheritance in each sample if emplaced 412ka ago
c)
462 ± 55 ka
(DN06S2 excluded)
235 ka
Surface and depth profile sample
Surface and depth profile sample with rejuvenation of 235 ka
Exposure of 235 ka (t min)
Amount of inheritance in each sample if emplaced 235 ka ago

Figure 5

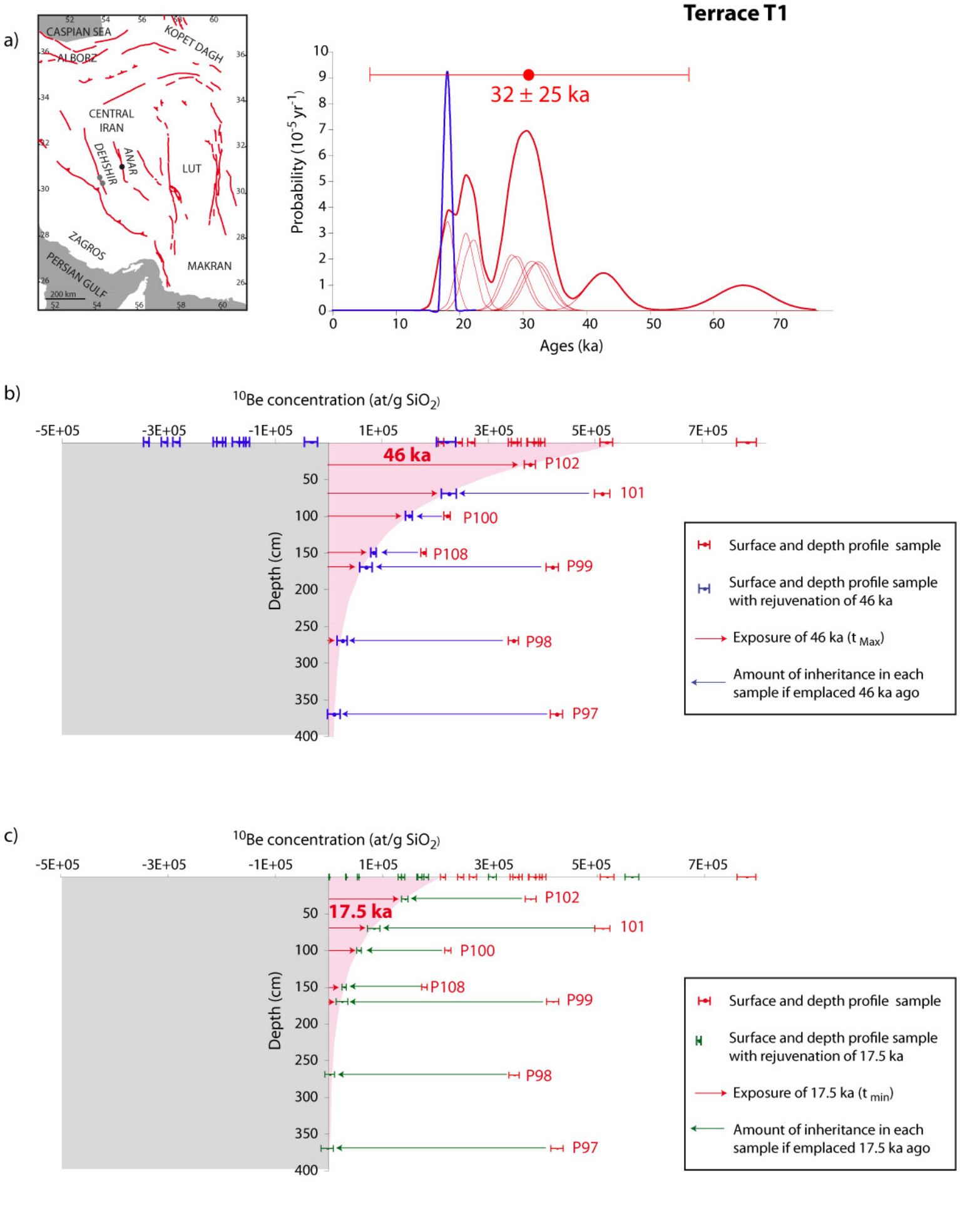
a)
CASPIAN SEA
KOPET DAGH
ALBORZ
CENTRAL IRAN
DEHSHIR
ANAR
LUT
ZAGROS
PERSIAN GULF
MAKRAN
200 km
Terrace T1
32 ± 25 ka
Probability (10^{-5} yr^{-1})
Ages (ka)
b)
^{10}Be concentration (at/g SiO_2)
46 ka
P102
101
P100
P108
P99
P98
P97
Depth (cm)
Surface and depth profile sample
Surface and depth profile sample with rejuvenation of 46 ka
Exposure of 46 ka (t_{Max})
Amount of inheritance in each sample if emplaced 46 ka ago
c)
^{10}Be concentration (at/g SiO_2)
17.5 ka
P102
101
P100
P108
P99
P98
P97
Depth (cm)
Surface and depth profile sample
Surface and depth profile sample with rejuvenation of 17.5 ka
Exposure of 17.5 ka (t_{min})
Amount of inheritance in each sample if emplaced 17.5 ka ago

Figure A1

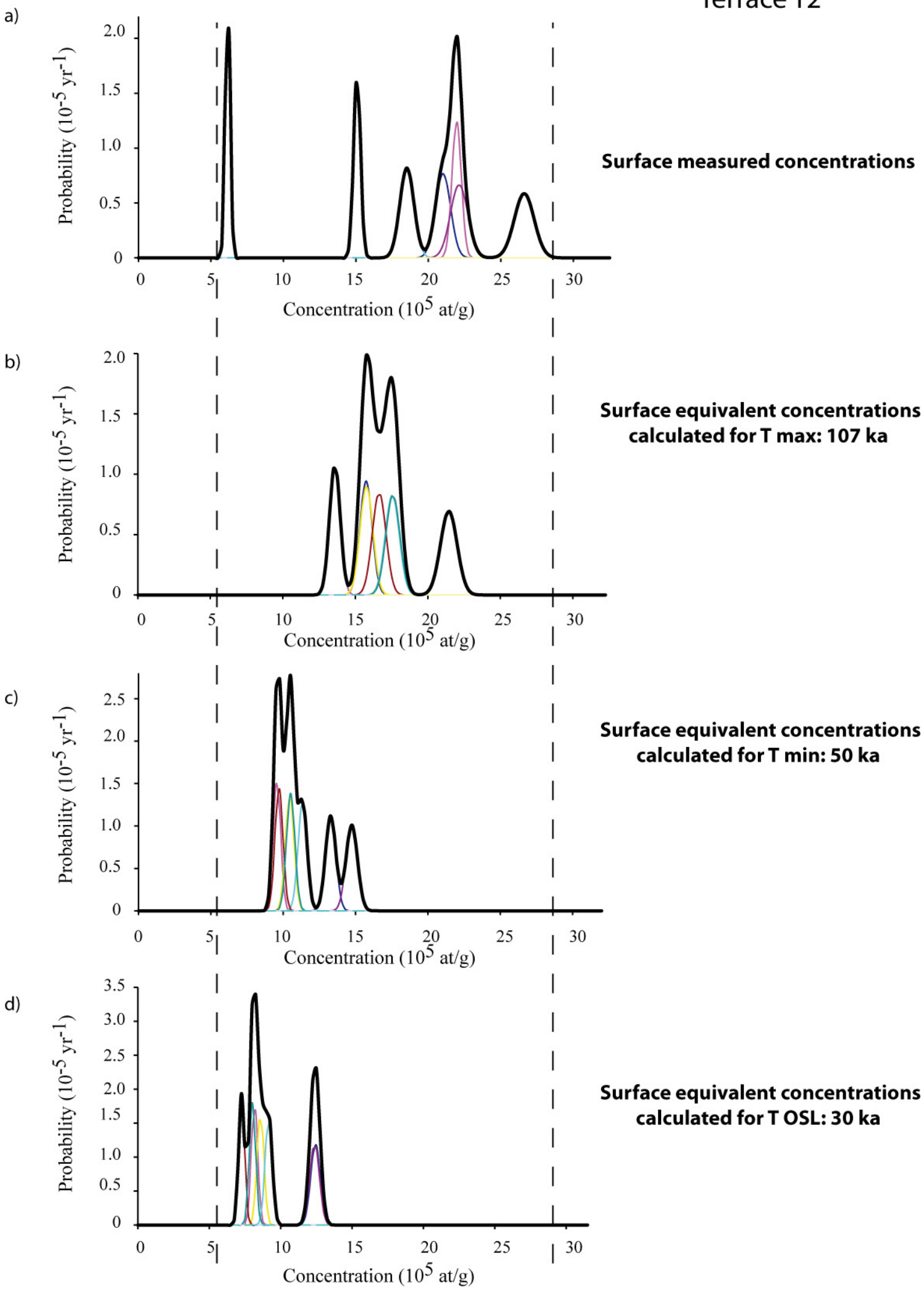
Terrace T2
a)
Probability (10^{-5} yr^{-1})
Concentration (10^5 at/g)
Surface measured concentrations
b)
Probability (10^{-5} yr^{-1})
Concentration (10^5 at/g)
Surface equivalent concentrations calculated for T max: 107 ka
c)
Probability (10^{-5} yr^{-1})
Concentration (10^5 at/g)
Surface equivalent concentrations calculated for T min: 50 ka
d)
Probability (10^{-5} yr^{-1})
Concentration (10^5 at/g)
Surface equivalent concentrations calculated for T OSL: 30 ka

Figure A2

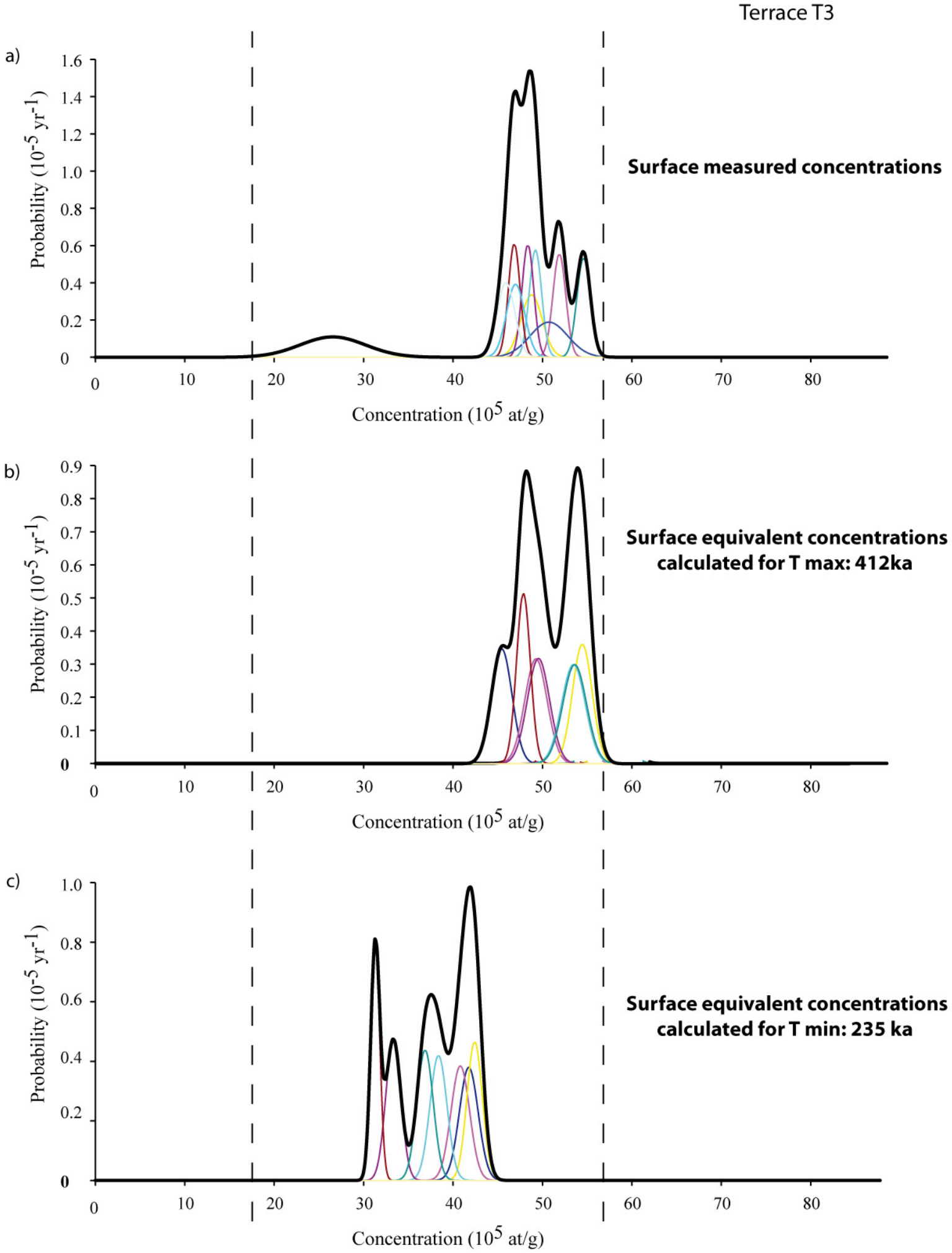
Terrace T3
a)
Probability (10^{-5} yr^{-1})
Surface measured concentrations
Concentration (10^5 at/g)
b)
Probability (10^{-5} yr^{-1})
Surface equivalent concentrations calculated for T max: 412ka
Concentration (10^5 at/g)
c)
Probability (10^{-5} yr^{-1})
Surface equivalent concentrations calculated for T min: 235 ka
Concentration (10^5 at/g)

Figure A3

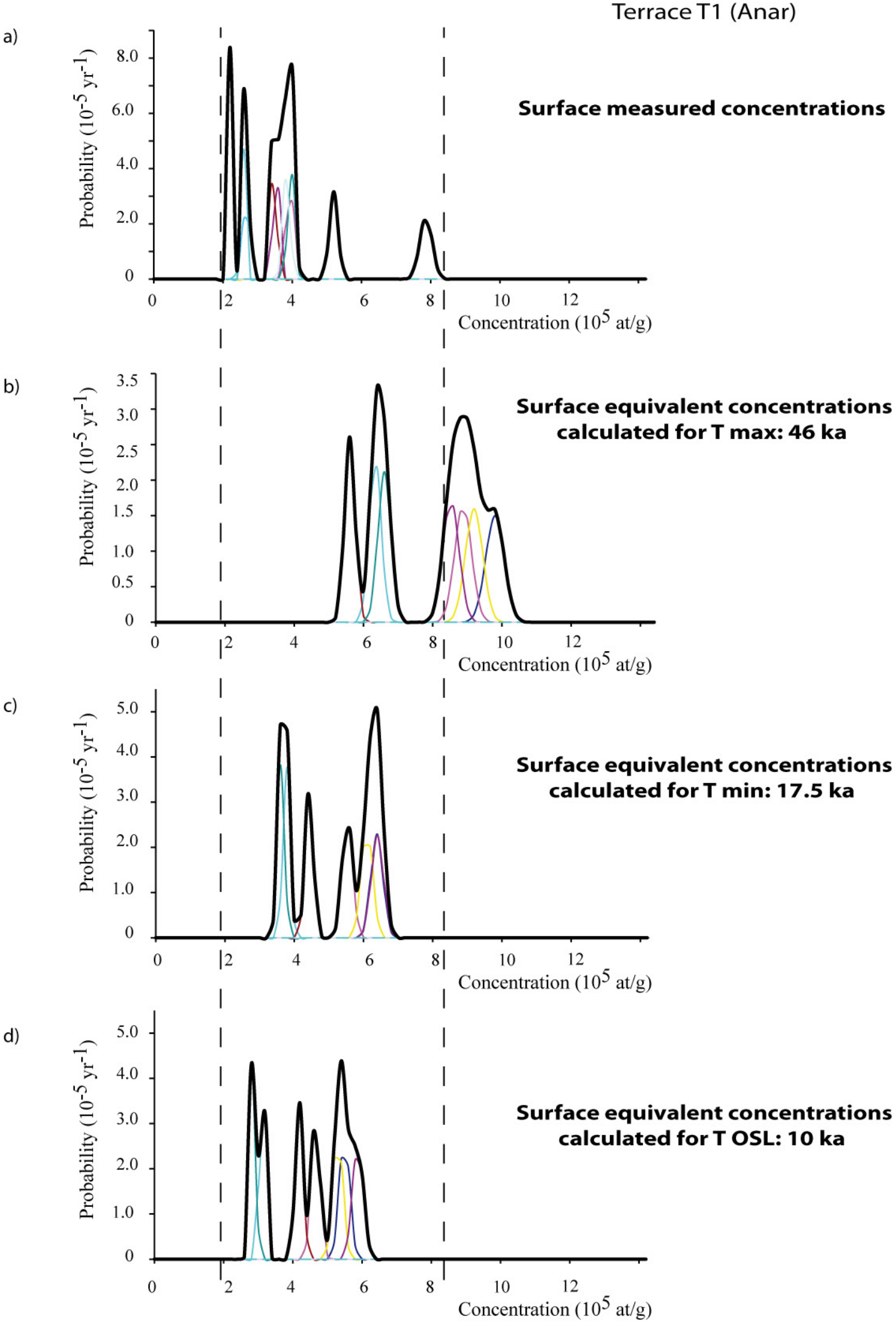
Terrace T1 (Anar)
a)
Surface measured concentrations
b)
Surface equivalent concentrations calculated for T max: 46 ka
c)
Surface equivalent concentrations calculated for T min: 17.5 ka
d)
Surface equivalent concentrations calculated for T OSL: 10 ka
Probability (10^{-5} yr^{-1})
Concentration (10^5 at/g)